Distinct immunopathological mechanisms of EBV-positive and EBVnegative posttransplant lymphoproliferative disorders

Cecilia Nakid-Cordero, Sylvain Choquet, Nicolas Gauthier, Noureddine Balegroune, Nadine Tarantino, Véronique Morel, Nadia Arzouk, Sonia Burrel, Géraldine Rousseau, Frédéric Charlotte, et al.

Distinct immunopathological mechanisms of EBV-positive and EBV-negative posttransplant lymphoproliferative disorders

Cecilia Nakid-Cordero[1], Sylvain Choquet[2], Nicolas Gauthier[1], Noureddine Balegroune[2], Nadine Tarantino[1,3], Véronique Morel[2], Nadia Arzouk[4], Sonia Burrel[5] Géraldine Rousseau[6], Frédéric Charlotte[7], Martin Larsen[1,3], Vincent Vieillard[1,3], Brigitte Autran[1], Véronique Leblond[2] and Amélie Guihot[1, 8] for the K-VIROGREF Study Group.

[1] Sorbonne Université (Univ. Paris 06), INSERM U1135, Centre d'Immunologie et des Maladies Infectieuses (CIMI-Paris), Hôpital Pitié-Salpêtrière, Paris, France; [2] Service d'Hématologie, Hôpital Pitié-Salpêtrière, Paris, France; [3] CNRS ERL8255, Centre d'Immunologie et des Maladies Infectieuses (CIMI-Paris), Paris, France; [4] Service de Néphrologie, Urologie et Transplantation Rénale, Hôpital Pitié-Salpêtrière, Paris, France; [5] Service de Virologie, Hôpital Pitié-Salpêtrière, Paris, France; [6] Service de Chirurgie Digestive, Hépato-Bilio-pancréatique et Transplantation Hépatique, Hôpital Pitié-Salpêtrière, Paris, France; [7] Service d'Anatomopathologie, Hôpital Pitié-Salpêtrière, Paris, France; [8] Département d'Immunologie, Assistance Publique-Hôpitaux de Paris (AP-HP), Groupe Hospitalier Pitié-Salpêtrière, Paris, France.

A complete list of the members of the K-VIROGREF Study Group appears in the "Appendix A".

Corresponding Author:

Amélie Guihot

Email: amelie.guihot@aphp.fr

ORCIDs:

Nakid-Cordero Cecilia (ORCID: 0000-0003-0722-7577)

ABBREVIATIONS

AICD, Activation-induced cell death

ADCC, Antibody-dependent cell cytotoxicity

CNS, Central nervous system

CTL, cytotoxic T-cell lines

EBER, EBV-encoded small RNA

EBV, Epstein-Barr virus

FDR, False discovery rate

FMO, Fluorescence minus one

OS, overall survival

PFS, progression-free survival

PTLD, Post-transplant Lymphoproliferative Disorder

PBMC, Peripheral blood mononuclear cells

ABSTRACT

EBV-positive and EBV-negative post-transplant lymphoproliferative disorders (PTLDs) arise in different immunovirological contexts and might have distinct pathophysiologies. To examine this hypothesis, we conducted a multicentric prospective study with 56 EBV-positive and 39 EBV-negative PTLD patients of the K-VIROGREF cohort, recruited at PTLD diagnosis and before treatment (2013-2019), and compared them to PTLD-free Transplant Controls (TC, n=21). We measured absolute lymphocyte counts (n=108), analyzed NK- and T-cell phenotypes (n=49 and 94) and performed EBV-specific functional assays (n=16 and 42) by multiparamenter flow cytometry and ELISpot-IFNγ assays (n=50). EBV-negative PTLD patients, NK cells overexpressed Tim-3; the 2-year progression-free survival was poorer in patients with a CD4 lymphopenia ($CD4^+$<300 cells/mm^3, p<0.001). EBV-positive PTLD patients presented a profound NK-cell lymphopenia (median=60 cells/mm^3) and a high proportion of NK cells expressing PD-1 (vs TC, p=0.029) and apoptosis markers (vs TC, p<0.001). EBV-specific T cells of EBV-positive PTLD patients circulated in low proportions, showed immune-exhaustion (p=0.013 vs TC) and poorly recognized the N-terminal portion of EBNA-3A viral protein. Altogether, this broad comparison of EBV-positive and EBV-negative PTLDs highlight distinct patterns of immunopathological mechanisms between these two diseases and provide new clues for immunotherapeutic strategies and PTLD prognosis.

1 INTRODUCTION

Post-transplant lymphoproliferative disorders (PTLDs) are heterogeneous tumors arising after solid-organ transplantation (SOT),[1] often related to the Epstein-Barr virus (EBV).[2] EBV-positive PTLD usually arise early after transplantation,[1,3] and are believed to result from altered NK- and T-cell responses against EBV-infected lymphocytes,[4] while the pathogenesis of EBV-negative PTLD is less clear.[1,5] EBV-positive and EBV-negative PTLDs might be related to distinct immunopathologies, but this has never been shown.

Described alterations in NK cells of EBV-positive PTLD patients include overexpression of NKG2A[6] and PD-1[7] inhibiting receptors, and down-regulation of NKp46 and NKG2D activating receptors,[6,7] suggesting a defective NK-cell functionality against EBV-positive PTLD. Yet, the respective contribution of NK-cell immunity during EBV-positive and EBV-negative PTLDs is not clear.

A general assumption is that impairment of EBV-specific T-cell responses lead to EBV-positive PTLD development.[4] Several studies have found similar proportions of IFNγ-producing EBV-specific $CD8^+$ T cells in EBV-positive PTLD patients compared to healthy donors[8,9] and transplant controls,[9] although those responses are mainly IFNγ-monfunctional in transplant recipients with and without PTLD.[10,11] The hypothesis that immune-exhaustion underlie EBV-specific T-cell impairment has only been studied in mice models[12] and transplant recipients carrying high EBV loads,[11,13] remaining to be characterized in both EBV-positive and EBV-negative PTLDs. Another hypothesis is that a low diversity of EBV-specific T-cell responses might contribute to EBV-positive PLTLD development. We recently showed that kidney transplant recipients carrying long-term stable EBV loads have a broader T-cell recognition of the latency III-protein

EBNA-3A than healthy individuals; a repertoire that might protect them against EBV-post-transplant complications,[14] mainly associated to type III latency.[15–17] One last hypothesis involves the role of EBV-specific $CD4^+$ T-cell responses, that have shown to be low in transplant recipients with[8,18] and without[14] EBV-positive PTLD. Moreover, EBV-positive PTLD patients show better clinical responses when infused with $CD4^+$ enriched EBV-cytotoxic T-cell lines (EBV-CTL).[19]

The development of adapted immunotherapiesrequires to better characterize the protective cellular responses against these two forms of PTLDs.[20–23] Here, we compare multiple immune-parameters of EBV-positive versus EBV-negative PTLD patients and PTLD-free transplant controls. We show distinct patterns of immunopathological mechanisms between EBV-positive and EBV-negative PTLDs and provide new clues for prospective surveillance and immunotherapeutic strategies.

2 MATERIALS AND METHODS

2.1 Study groups

We conducted a multicenter, prospective study of ninety-five adult SOT recipients diagnosed with PTLD from March 2013 to November 2019. Patients were recruited across 20 French medical centers through the K-VIROGREF (virus-induced cancers after transplantation) Study Group, at diagnosis and before reduction of immunosuppression or any immuno/chemo-therapy (Figure 1). PTLD diagnosis, including assessment of tumor EBV status (by *in situ* hybridization of EBV-encoded small RNA (EBER)), was performed by hematopathology at the respective institutions. Included patients were classified as EBV-pos (n=56) or EBV-neg (n=39) according to

EBV status of the tumor (Figure 1). PTLD-free transplanted controls (TC, n=21) were prospectively recruited from the renal (n=10)[14] and hepatic (n=5) transplantation services of the Pitié-Salpêtrière Hospital (Paris, France) or retrospectively included (n=5 liver and 1 kidney) from the K-GREF cohort[24,25](Supplemental methods and Figure S1).

This study was approved by institutional research ethics board, Comité de Protection des Personnes Ile-de-France VII (no°PP13-022) and performed in accordance with the human-experimentation guidelines of the declaration of Helsinki. All patients provided written informed consent.

2.2 Blood samples

Blood samples were obtained at patient inclusion and centralized at the Department of Immunology of the Pitié-Salpêtrière Hospital were tests were performed except for the EBV PCR, which was tested in whole blood by Virology departments at each center. Absolute T/B/NK lymphocyte counts were determined in whole blood with an automated AQUIOS CL flow cytometry system (Beckman Coulter, Villepinte, France)

2.3 NK-cell phenotype and functional assays

NK-cell phenotypes including differentiation (CD56, CD16, CD57), expression of c-lectin (NKG2A, NKG2C), natural cytotoxicity (NKp30, NKp46) and killer immunoglobulin receptors (Kir2DL2/3, Kir3DL1), immune-checkpoints (PD-1, Tim-3) and apoptosis markers (caspase-3, FAS), were assessed in thawed PBMCs. For NK-cell functional assays,[26] PBMCs were incubated overnight at 37°C, 5% CO_2 with or

without IL-12 (10ng/mL) and IL-18 (100ng/mL; RD systems), then stained with anti-CD107a-FITC (BD Biosciences) an incubated for 6 hours with media or K562 targets (E:T ratio of 1:1). After 1-hour incubation, BD GolgiStop/GolgiPlug were added according to manufacturer instructions (BD Biosciences). Cells were stained as mentioned above. The anti-active caspase-3-FITC and anti-IFNγ-AF700 (Becton Dickinson) were added after cell-permeabilization (Cytofix/Cytoperm™; BD Biosciences). At least 2000 live $CD3^{-}CD56^{+}$ NK cells were acquired with a Gallios flow cytometer (Beckman Coulter). Positive populations were designed with FMO controls. All antibodies are detailed in supplemental methods.

2.4 T-cell phenotype and functional assays

T-cell differentiation (CCR7, CD45RA and CD57) and activation (CD25, CD38, HLA-DR, CD95) phenotypes were determined in whole blood with a Navios Flow Cytometer (Beckman Coulter). T-cell immune-checkpoints expression (PD-1 and TIM-3) was assessed in thawed PBMCs with a LSR Fortessa Flow Cytometer (BD Biosciences).

For EBV-specific T cell detection, thawed PBMCs were incubated for 6 hours with HLA-restricted and BZLF-1 EBV peptides (2µg/mL), Staphylococcal enterotoxin B (1µg/mL; Sigma-Aldrich) or media in presence of brefeldin A (10µg/mL) and monensin (5µg/mL; Sigma-Aldrich). Cells were stained as mentioned above, then permeabilized and stained for intracellular cytokine detection (IFNγ, IL-2, TNFα). Samples were acquired with a LSR Fortessa. EBV-specific T cells were detected in a Boolean OR gate ($IFN\gamma^{+}$, $IL\text{-}2^{+}$, $TNF\alpha^{+}$), based on unstimulated and FMO controls, within live $CD3^{+}CD4^{+}$/$CD3^{+}CD8^{+}$ lymphocytes. Results are reported after background subtraction. Immune-checkpoint expression was analyzed in populations larger than

100 cell-events. ELISpot-IFNγ assays were performed as previously described.[14] EBV-peptides and antibodies are described in supplemental methods and Tables S1-S4.

2.5 Immunohistochemistry

The CD3/CD4/CD8/PD-L1 immunostaining procedure was performed on 2 formalin fixed and deparaffinized tumor sections as described in supplemental methods.

2.6 Statistical Analysis

Flow cytometry data were analyzed with FlowJo 10.6 (Tree star, USA). Statistical analysis were performed in GraphPad Prism 6 (La Jolla, USA) and Rstudio 1.3. Chi-square, two-tailed Mann-Whitney or two-tailed Kruskal-Wallis tests were used when appropriate. Correlations were determined with the Spearman rank correlation coefficient. Kaplan-Meier curves were compared with log-rank test. Survival was calculated from the date of PTLD diagnosis to the date of death or last follow-up for Overall survival (OS) or to the date of disease progression/ death or last follow-up.for Progression-Free survival (PFS). Continuous variables were dichotomized using median values from all available measures or previously published[27] cut-off values to compare patients outcome. Cox-regression analysis are described in supplemental methods. P-values are reported after Multiplicity adjustment with Dunn's post-test or with false discovery rate correction (FDR=0.05) as specified.

3 RESULTS

3.1 Patients Characteristics

Fifty-six EBV-pos and 39 EBV-neg PTLD patients were included at initial diagnosis (Figure 1). Median time from last transplantation to diagnosis was 7.5 years for EBV-pos and 10 years for EBV-neg PTLDs (Table 1; Figure S2A)]. CNS involvement was observed in 30 PTLDs (31%), a larger proportion than previous reports in France and European countries (8-21%)[28–30]. All CNS-PTLD cases were primary (pCNS, n=30), had late (73% >5years post-SOT) or very late onset (43% >10years post-SOT) and were EBV-related (97%), possibly explaining the late median occurrence of EBV-pos PTLDs in our cohort. Included controls (TC, n=21) did not differ for sex, age and immunosuppressive regimens (Table 1). The median follow-up after PTLD diagnosis was 5 months (min-max, 0-57) for EBV-pos and 14 months (min-max, 0-56) for EBV-neg. On January 2020, 32 patients were deceased (TC n=0, EBV-pos n=17, EBV-neg n=15). Main causes of death were PTLD progression (n=19), septic shock (n=4), cardiovascular/respiratory complications (n=3) and hepatic failure (n=1). Overall survival (OS) and progression-free survival (PFS) were not different for EBV-pos vs EBV-neg PTLDs (Figure S2B-C). Noteworthy, EBV-pos patients with pCNS-PTLD had similar OS and PFS than systemic-PTLD (Figure S3).

3.2 $CD4^+$ T-cell lymphopenia impacts the 2 year-survival of EBV-negative PTLD patients

Next, we examined how lymphopenia impact EBV-pos or EBV-neg PTLD outcomes, by considering median lymphocyte counts (108 individual measures) as cut-off value. EBV-pos carried lower absolute lymphocyte counts than TCs (P=0.007; Figure 2A) but had similar 2-year OS and PFS whatever the degree of lymphopenia (Figure 2C and

S4B), while lymphopenic (<900 cells/mm^3) patients at EBV-neg PTLD diagnosis had inferior 2-year OS and PFS than EBV-neg patients without lymphopenia (14% vs 62%; P=0.076; Figure 2B and S4A). We further studied PTLD outcome in relation with each lymphocyte subtype. EBV-neg patients with CD4 lymphopenia (<300 cells/mm^3) at PTLD diagnosis had significantly poorer OS and PFS than EBV-neg patients without CD4 lymphopenia (11% vs 61%; P<0.001; Figure 2E and S4C), while this parameter showed no association to EBV-pos PTLD outcome. (Figure 2F and S4D). NK-cell counts were significantly lower in EBV-pos compared to both TC and EBV-neg groups (P<0.001 and P=0.024; Figure 1G) but did not impacted outcome of any PTLD group (Figure 1H-I). Time since last transplantation showed no association with lymphocyte subset counts at inclusion (data not shown).

Altogether, these results suggest that CD4$^+$ T-cell counts could be useful as a prognosis marker of EBV-neg PTLD whereas the NK-cell compartment may be of interest for the understanding of EBV-pos PTLDs immunopathology.

3.3 High activation-induced cell death of NK cells during EBV-positive PTLD

We next explored the mechanisms of the NK-cell lymphopenia observed in PTLD patients. First, it involved both CD56^{Bright} and CD56^{Dim} subsets (Figure S5A). EBV-pos and EBV-neg patients presented similar NK-cell phenotypes than TCs in terms of expression of CD57, c-lectin receptors (NKG2A and NKG2C), natural cytotoxicity receptors (NKp30 and NKp46) and killer immunoglobulin receptors (Kir2DL2/3 and Kir3DL1)(Figure S5A). The early activation marker CD69 was overexpressed on NK cells from both EBV-pos and EBV-neg patients (vs TC, P<0.001and P<0.001), with superior expression of late activation marker HLA-DR on NK cells of EBV-pos (vs TC,

P=0.001) (Figure 3A). EBV-pos patients who underwent post-transplant EBV-primary infection had the highest proportions of activated NK cells (data not shown). Co-expression of CD69 and HLA-DR was also increased in both PTLD groups (Figure S5B). The HLA-DR MFI on total NK cells negatively correlated with NK-cell absolute counts among all groups (Rho=-0.6809, P<0.001; Figure S5C). Moreover, NK cells from EBV-pos patients expressed higher levels of PD-1 than the other groups (vs TC, P=0.029; vs EBV-neg PTLD, P=0.025; Figure 3B), supporting the hypothesis that increased NK-cell activation might lead to cellular exhaustion. The significantly higher EBV loads in EBV-pos (vs TC, P=0.002; vs EBV-neg, P=0.001; Table 1) positively correlated with high proportions of PD-1$^+$ NK cells (Rho=0.5624, P=0.015, Figure 3C). Conversely, the EBV-neg group displayed higher TIM-3 expression on NK cells (vs EBV-pos P=0.001, Figure 3B), suggesting different mechanisms for NK-cell lymphopenia in EBV-pos and EBV-neg PTLDs.

To explore whether NK-cell lymphopenia result of increased activation-induced cell death (AICD), we measured NK-cell expression of the death receptor FAS (CD95)[31] and the active form of caspase-3.[32] As expected, EBV-pos and EBV-neg groups presented higher frequencies of active-caspase-3$^+$ (P<0.001 and P=0.002) and active-caspase-3$^+$ Fas$^+$ NK cells (P<0.001 and P=0.005), compared to TCs (Figure 3D). NK cells from EBV-pos patients expressed significantly higher levels of FAS than TCs (P=0.040, Figure 3D), suggesting that a larger number of NK cells potentially undergo AICD in those patients.

We further studied NK-cell functional capacity at PTLD diagnosis by performing cytokine production and degranulation assays in patients with matched NK-cell counts at diagnosis. The proportion of IFNγ$^+$ NK cells after IL-12/IL-18 stimulation and of CD107a$^+$ NK cells after incubation with K562 targets were similar between both PTLD

groups and TCs (Figure S5E). Interestingly, patients with lower-median counts (<90 NK cells/mm^3) had significantly higher frequencies of IFNγ$^+$ NK cells than patients with upper-median counts (>90 NK cells/mm^3; P=0.042, Figure 3E), whatever the groups. The frequency of IFNγ$^+$ NK cells from all groups positively correlated with EBV loads (Rho=0.6694; P=0.014, Figure 3F) while IFNγ$^+$ NK cells from EBV-pos showed higher PD-1 expression compared to TC patients (P=0.034; Figure 3G).

Altogether, these data link the high EBV loads observed in EBV-pos PTLDs with NK-cell activation, PD-1 expression and depletion, in line with a poor tumor immune control.

3.4 High proportions of CD4$^+$ TIM-3$^+$ T cells at EBV-negative PTLD diagnosis are associated with poor clinical outcome

To better understand the relation between CD4$^+$ lymphopenia and EBV-neg PTLD outcome, we conducted a detailed analysis of T-cell phenotypes. Considering the distribution of naïve and memory subsets (CCR7 and CD45RA) and the expression of activation (CD25 and HLA-DR) and pro-apoptotic (FAS) markers, CD4$^+$ and CD8$^+$ T-cell phenotypes were similar between the three groups (Figures 4A, S6-S7). The proportion of PD-1$^+$ CD4$^+$ T cells was increased in EBV-pos compared to TCs (P=0.031; Figure 4B), while the proportions of TIM-3$^+$ CD4$^+$ (vs TC, P<0.001 and P<0.001; Figure 4C) and of PD1$^+$ TIM-3$^+$ CD4$^+$ T cells were increased in both EBV-pos and EBV-neg groups (vs TC, P<0.001 and P<0.001; Figure 4D). As high proportions of Tim-3$^+$ CD4$^+$ T cells correlated with low CD4$^+$ T-cell counts at EBV-neg PTLD diagnosis (Rho=-0.5300, p=0.001; Figure S6D), we next studied the relation of this parameter with PTLD outcome. EBV-neg patients carrying >5% of TIM-3$^+$ CD4$^+$ T cells

at diagnosis had lower PFS (18% vs 70%; Figure 3E) and OS (Figure S6G) than patients with <5% TIM-3$^+$ CD4$^+$ T cells, although statistical significance (P=0.0339) was lost after FDR correction (P=0.1017). Noteworthy, a similar trend was observed when analyzing only EBV-neg DLBCL tumors (data not shown). We next examined the prognostic value of CD4$^+$ T-cell counts, %TIM-3$^+$ CD4$^+$ T cells and previously described prognostic factors for PTLDs.[29,33] In univariate analysis, only age (HR=0.28, p=0.032) and CD4 lymphopenia (HR=0.1, p=0.002) at EBV-neg PTLD diagnosis had a significant effect over OS (Table S5). Both values remained significant in multivariate cox-regression model, confirming their independent prognostic value for OS of EBV-neg PTLDs (Table S6).

The CD8$^+$ T-cell phenotype showed high frequencies of activated CD38$^+$HLA-DR$^+$ CD8$^+$ T cells (vs TCs, P=0.008 and P=0.017; Figure 4G) in EBV-pos and EBV-neg groups, without significant association with EBV loads (data not shown). The proportion of PD-1$^+$ CD8$^+$ T cells was similar between groups (Figure 4H), though both EBV-pos and EBV-neg showed increased PD-1 MFI on total CD8$^+$ T cells (Figure S7F). The proportions of TIM-3$^+$ CD8$^+$ (vs TC; P<0.001 and P<0.001, Figure 4I) and of PD1$^+$ TIM-3$^+$ CD8$^+$ T cells were also increased in EBV-pos and EBV-neg (vs TC; P<0.001 and P<0.001; Figure 4J).

Taken together, these data show CD8 activation during EBV-pos PTLD and a distinct pattern of CD4$^+$ T-cell immune-exhaustion during EBV-pos and EBV-neg PTLDs.

3.5 EBV-specific CD8$^+$ T cells are exhausted at EBV-positive PTLD diagnosis

To gain further insight in EBV-pos PTLD immunopathology, we next evaluated EBV-specific T-cell responses against latent and lytic EBV peptides (MHC-I/-II restricted and

BZLF-1) using IFNγ, IL-2 and TNFα intra-cytoplasmic staining and a 3 cytokine boolean strategy to detect total EBV-specific T cells. EBV-specific $CD4^+$ T-cell responses were low in all three groups, but the ratio between EBV-specific $CD4^+$ T cells and EBV DNA was lower in EBV-pos patients (Figure S8A). The low proportions of EBV-specific $CD8^+$ T cells (Figure 5A) observed in EBV-pos patients also resulted in a reduced EBV-specific $CD8^+$ T cells/EBV DNA ratio (vs TC; P=0.008; Figure S8B). Furthermore, EBV-pos patients had increased proportions of PD-1^+ (vs TCs; P=0.029) and PD-1^+TIM-3^+ (vs TCs; P=0.013) EBV-specific $CD8^+$ T cells (Figure 5B). We next examined the tumor microenvironment in two patients. PD-L1 expression was higher in the EBV-pos (90%) than in the EBV-neg (30%) tumor (Figure 6E-F). The $CD3^+$ T-cell infiltration was low in both tumors (10%; Figure 6G-H) mainly composed (80%) of $CD8^+$ cells in the EBV-pos but only 30% in the EBV-neg PTLD (Figure 6I-J). Altogether, these data suggest that $CD8^+$ T cells are already exhausted and low-numbered against EBV at EBV-pos PTLD diagnosis but migrate to the tumor.

3.6 EBV-pos patients have low diversity of EBNA-3A-specific T-cell responses

We next evaluated the diversity of EBV-specific T-cell responses against different peptide pools covering latent and lytic EBV immunodominant proteins by ELISpot-IFNγ assay. As expected,[8,14,18] $CD4^+$ T-cell responses against class II-MHC restricted EBV peptides were barely detected, with only 5/11, 3/4 and 5/8 responders in TC, EBV-pos and EBV-neg groups, respectively (Figure 5C). $CD8^+$ T-cell responses against the class I-MHC restricted, BZLF-1 and EBNA-3A EBV peptides were highly detectable among 46/50 tested patients except for four EBV-pos patients who did not respond to any peptide pool (Figure S8C). EBV-specific T cells from the EBV-pos group barely recognized the N-terminal region of the EBNA-3A sequence (Pools 1-4; n=1/18),

containing the EBNA-3 family homology region[34] (Pools 1-4 out of 16; AA position 133-313) while both TCs (pools1-4; n=6/12) and EBV-neg (pools1-4; n=7/20) widely recognized this region (Figure 5C). Noteworthy, we observed that 100% of pCNS EBV-pos PTLD patients (n=9) had undetectable T cell responses against EBNA-3A, while 40% (n=4) of tested (n=9) systemic EBV-pos PTLD patients had detectable responses against EBNA-3A (Figure S9), most of whom had a positive pre-transplant EBV-serology. Mapping of predicted and detected responses according to patients HLAs did not show allele-related patterns (Tables S7 and S8). Further comparison of the proportional contribution of EBNA-3A or BZLF-1 specific T-cell responses showed a bias in favor of lytic BZLF-1 protein recognition in the EBV-pos group, while the responses of TCs and EBV-neg were equally distributed (Figure 5D). Altogether, these results show a lack of recognition of the EBNA-3A sequence by the effector/effector memory EBV-specific T cells at EBV-pos PTLD diagnosis, with a shift in the repertoire of the response from latent to lytic EBV proteins.

4 DISCUSSION

Although increasing evidences show dissociating patterns for EBV-positive and EBV-negative PTLDs,[1,5,35–38] immune characteristics of PTLDs had rarely been studied according to the EBV status of the tumor.[39] Here, we suggest distinct immunopathological mechanisms for these two diseases that could influence the development of different prognostic markers and therapeutic strategies for PTLDs according to their association with EBV.

Several prognostic factors of PTLDs have been previously described, including older age,[27,29] high LDH levels[29] and global lymphopenia[33,40] However, their specific relevance for EBV-pos or EBV-neg tumors has never been studied, leading to the description of prognostic markers for PTLDs in their globality that could be associated to the immunopathology underlying the presence or not of EBV. Our data show that CD4 lymphopenia and older age are specifically associated with poor prognosis of EBV-neg PTLDs. Given that $CD4^+$ T-cell counts can be easily monitored in a routine basis, larger studies evaluating their prognostic value at EBV-neg PTLD diagnosis should be considered.[41] We also observed that EBV-neg patients with poor PFS also presented the highest proportions of TIM-3^+ $CD4^+$ T cells. Similar to previous reports in NHL of immunocompetent patients[42], which generally are EBV-negative.[43] In our study, NK cells from EBV-neg PTLDs also over-expressed TIM-3, an immune-checkpoint normally expressed by mature[44] and exhausted[45–49] NK cells, the anti-tumoral functions of which can be reversed after TIM-3 antagonisation.[49] TIM-3 overexpression by both NK and $CD4^+$ T cells could be involved in the physiopathology of EBV-neg PTLDs, although our results do not allow us to conclude whether those parameters are at the origin of disease progression or rather a consequence.

We describe for the first time an NK-cell lymphopenia at PTLD diagnosis. The high expression of AICD markers we observed on NK cells from EBV-pos and EBV-neg patients suggests AICD might be involved in the peripheral depletion of NK cells, although we cannot exclude the possibility of a large migration of NK cells to the tumor could result in NK-cell lymphopenia. NK cells of EBV-pos patients expressed high levels of PD-1, as previously reported in kidney recipients with chronic EBV loads[14] and EBV-positive PTLD pediatric patients in whom NK-cell function was recovered *in-*

vitro after PD-1/PD-L1 blockade.[7] In our study, the NK-cell cytotoxicity was not altered in EBV-pos patients but high frequencies of IFNγ^{+} NK cells were associated with high EBV loads in NK-cell-lymphopenic patients, suggesting excessive activation might lead to peripheral NK-cell depletion. Our data links PD-1 expression by NK cells to EBV antigenic hyperstimulation; a phenotype that might be enhanced in patients who underwent post-transplant primary EBV-infection. Indeed, NK-cell hyperactivation probably contribute to EBV-pos PTLD immunopathology, partially explaining the early occurrence of the disease in pre-transplant EBV-seronegative patients. Our findings encourage the development of NK-cell immunotherapies to treat EBV-positive PTLD, such as adoptive transfer of activated NK cells[50] or CAR-transduced NK cells.[51] Besides, the NK-cell lymphopenia we report at PTLD diagnosis constitute a rational to study rituximab resistance in both EBV-positive and EBV-negative PTLD patients, accounting that rituximab-based therapies relay on NK-cell mediated ADCC of transformed-B-cells.[52]

Our results also show low proportions of EBV-specific CD8^{+} T cells in EBV-pos PTLD patients, suggesting a similar mechanism as for HHV-8, another gamma-herpesvirus.[53] Accounting that EBV-positive PTLDs are generally BZLF-1-negative tumors[15] except for few reported cases of pCNS-PTLD,[17,54] the skewing of T-cell responses against the BZLF-1 lytic protein in EBV-pos patients could reflect peripheral EBV reactivation[55] and/or low recognition of tumoral EBNA-3A latent protein. EBV-positive PTLDs generally express EBNA-3A[17] and a broad T-cell recognition of the EBNA-3A N-terminal might have a protective role against EBV-positive PTLDs.[14] Besides, all EBV-positive pCNS-PTLD patients had undetectable T-cell responses against EBNA-3A. These results suggest that therapies based on the infusion of EBV-CTL could be enriched with EBNA-3A-specific T cells, as those cells seem to be protective in our

study. Another hypothesis is that EBNA-3A-specific T cells might migrate to the tumor and become functionally exhausted. We observed that $CD8^+$ cells dominated the T-cell infiltrate in the EBV-pos PTLD microenvironment and that tumor cells highly expressed PD-L1,[56,57] while peripheral EBV-specific $CD8^+$ T cells overexpressed PD-1/Tim-3.[58] The low latent EBV-specific Th1 $CD4^+$ T-cell responses generally observed in transplanted patients[8,14,18] are another factor that might difficult the establishment of protective $CD8^+$ T-cell responses in EBV-seronegative patients, while limiting the acquisition of protective repertoire in EBV-seropositive patients. The alterations of EBV-specific T-cell responses we report provide new insights in the immunopathology of EBV-positive PTLDs and could promote the development of innovating immunotherapies, such as adoptive EBV-specific T-cell transfer[20,21,59] and therapeutic vaccination.[60,61]

Finally, we propose a model of EBV-pos and EBV-neg PTLD immunopathologies, based on these experimental findings and previously published results[14] (Figure 7). Briefly, following transplantation and immunosuppressive treatment, the $CD4^+$ Th1 response to latent EBV is hampered but might be compensated by the development of a protective repertoire of EBNA-3A-specific $CD8^+$ T-cell responses that control EBV-driven B-cell transformation. EBV-positive PTLDs arise in a context where Th1 responses against latent EBV are low and $CD8^+$ T-cell responses poorly recognize the N-terminal portion of the viral protein EBNA-3A. NK cells and EBV-specific $CD8^+$ T cells circulate at low proportions, are highly activated and overexpress PD-1, while the tumor microenvironment presents $CD8^+$ T-cell infiltration, which may be exhausted meeting their PD-1 ligand expressed by tumor cells. Early development of EBV-positive PTLD might be accelerated in SOT recipients undergoing primary EBV-infection, who present higher NK-cell activation possibly leading to increased AICD,

while the establishment primary CD8+T cell responses lack proper Th1 help. During EBV-neg PTLD, $CD4^+$ lymphopenia and abundant peripheral TIM-3^+ $CD4^+$ T cells are associated with disease evolution, while TIM-3 overexpression by NK cells and $CD4^+$ T cells might contribute to EBV-negative PTLD immunopathology.

A major strength of this work is our K-VIROGREF cohort, the largest PTLD cohort in France, who allowed us to describe specific alterations of T-cell and NK-cell immunity for EBV-pos and EBV-neg PTLDs. Limitations of our study include a single blood-sample at inclusion, generalizability of PTLD subtypes and missing pre-transplant EBV-serology of 30% of patients and controls. The generalizability of different PTLD subtypes with different morphologies and localizations might overlap different immunopathological scenarios. In particular, EBV-pos pCNS-PTLDs were overrepresented in our cohort[28–30] and seemed to share common aspects with systemic cases, but different patterns of cellular mRNA and lytic-EBV gene expression between pCNS and systemic PTLD have been reported,[17,54] suggesting that two potentially different scenarios could exist. Another aspect we could only partially explore is the specific impact of post-transplant EBV primary-infection or reactivation over the NK and T cell alterations observed in EBV-pos PTLDs. Larger prospective studies exploring the impact of pCNS vs systemic localization and the evolution of our observations before and after PTLD diagnosis are greatly encouraged.

This broad comparison of T-cell and NK-cell characteristics between EBV-positive and EBV-negative PTLDs highlight distinct patterns of immunopathological mechanisms between these two diseases and provide new clues for prospective surveillance and immunotherapeutic strategies.

ACKNOWLEDGMENTS

This study was supported by INCA-DGOS-Inserm_12560 : SiRIC CURAMUS is financially supported by the French National Cancer Institute, the French Ministry of Solidarity and Health and Inserm with financial support from ITMO Cancer AVIESAN (Alliance Nationale pour les Sciences de la Vie et de la Santé/ National Alliance for Life Sciences & Health). This work was also supported by a PhD grant (C.N.-C; TAQK18773) from La Ligue contre le cancer (www.ligue-cancer.net).

The authors would like to thank the Study of Cancers After Solid Organs Transplants (K-GREF) study group for sharing data and samples of transplant controls and Dormeur Investment Service Ltd. that provided funding to purchase the plate reader used for the ELISpot-IFNγ assay.

They also thank Christophe Parizot, the T4/T8 department, Alice Rousseau, Catherine Blanc and the staff of the Flow Cytometry Core CyPS (Sorbonne University, Pitié-Salpêtrière Hospital, Paris, France) for technical help, as well as Guislaine Carcelain for providing latent EBV peptides.

DISCLOSURE

The authors of this manuscript have no conflicts of interest to disclose, as described by the *American Journal of Transplantation.*

DATA AVAILABILITY STATEMENT

For original data, please contact the corresponding author.

APPENDIX A: K-VIROGREF Study Group members.

Pr Véronique LEBLOND, Dr Véronique MOREL, Dr Sylvain CHOQUET, Dr Noureddine BALEGROUNE, Service d'Hématologie clinique, Hôpital Pitié-Salpêtrière-APHP, Paris; Dr Stéphane BARETE, Service de Dermatologie , Hôpital Pitié-Salpêtrière-APHP, Paris; Pr Céleste LEBBE, Service de Dermatologie , Hôpital Saint-Louis-APHP, Paris; Dr Morgane CHEMINANT, Service d'Hématologie adulte, Hôpital Neker-enfants malades-APHP, Paris; Pr Camille FRANCES,, Service de Dermatologie et Allergologie , Hôpital Tenon-APHP, Paris; Dr Rémy DULERY, Service d'Hématologie clinique et thérapie cellulaire, AP-HP Saint Antoine, Paris; Pr Catherine THIEBLEMONT , Service d'onco-hématologie, Hôpital Saint-Louis, Paris; Dr Maren BURBACH, Service de Néphrologie-Transplantations, Hôpital Saint-Louis, Paris; Dr Ali DADBAN, Service de Dermatologie , CHU d'Amiens-Picardie, Amiens; Dr Amandine CHARBONNIER, Hématologie Clinique et Thérapie Cellulaire, CHU d'Amiens-Picardie, Amiens; Dr Yannick LECORRE , Service de Dermatologie et vénéréologie, CHU d'Angers, ANGERS; Dr Marie-Pierre MOLES, Service d'Hématologie, CHU d'Angers, ANGERS; Pr François AUBIN, Service de Dermatologie, Maladies Sexuellement Transmissibles, Allergologie Et Explorations Cutanées, Hôpital Jean Minjoz, Besançon; Dr Adrien CHAUCHET, Dr Annie BRION, Service d'Hématologie, Hôpital Jean Minjoz, Besançon; Dr Anne PHAM-LEDARD, Service de Dermatologie et dermatologie pédiatrique, CHU de Bordeaux, Bordeaux; Pr Marie BEYLOT-BARRY, Service de Dermatologie et dermatologie pédiatrique, CHU de Bordeaux, Bordeaux; Dr Kamal BOUABDALLAH, Service d'Hématologie et thérapie cellulaire., CHU de Bordeaux, Bordeaux; Pr Lionel COUZI, Service de Néphrologie-transplantation-dialyse-aphérèses, CHU de Bordeaux, Bordeaux; Dr Fontanet BIJOU, Service d'Hématologie Clinique, Institu Bergonié, Bordeaux; Pr Laurence VERNEUIL, Service de Dermatologie , CHU Caen, Caen; Pr Gandi Laurent DAMAJ, Service d'Hématologie, CHU Caen, Caen; Dr Nicolas BOUVIER, Service de néphrologie-dialyse-transplantation rénale., CHU Caen, Caen; Dr Juliette BOUTELOUP, Service d'Hématologie-Oncologie, Centre hospitalier Chalon sur Saône, Chalon-sur-Saône; Dr Cécile MOLUCON-CHABROT, Service de Thérapie cellulaire et Hématologie, CHU Estaing, Clermont-Ferrand; Pr Corinne HAIOUN, Service d'Hématologie Lymphoïde, Hôpital Henri-Mondor -APHP, Creteil; Dr Laurence LE CLEACH, Service d'Hématologie Lymphoïde, Hôpital Henri-Mondor -APHP,

Creteil; Dr Sophie DALAC, Service de Dermatologie , CHU de Dijon , Dijon; Dr René-olivier CASASNOVAS, Service d'Hématologie Clinique, CHU de Dijon , Dijon; Dr Eileen BOYLE, Service d'Hématologie Clinique, Hôpital Claude Huriez, Lille; Dr Sébastien DHARANCY, Service d'Hématologie Clinique, Hôpital Claude Huriez, Lille; Dr Arnaud JACCARD, Service d'Hématologie clinique et thérapie cellulaire, CHU de Limoges, Limoges; Dr Anne-Sophie MICHALLET, Service d'Hématologie Clinique, Centre Léon Berard, Lyon; Dr Yann GUILLERMIN, Service d'Hématologie Clinique, Centre Léon Berard, Lyon; Dr Emmanuel BACHY , Service d'Hématologie clinique, Centre hospitalier Lyon sud, Lyon; Dr Hervé GHESQUIERES, Service d'Hématologie clinique, Centre hospitalier Lyon sud, Lyon; "Dr Emmanuel MORELON, Service de transplantation, néphrologie et immunologie clinique, Hôpital Edouard Herriot, Lyon; Dr Laure FARNAULT DE LASSUS, Service d'Hématologie, Hôptal de la conception, Marseille; Dr Vadim YVANOV, Service d'Hématologie, Hôptal de la conception, Marseille; Dr Stéphane FAURE, Service Hépato-gastro-entérologie, CHU de Montpellier, Montpellier; Pr Bernard GUILLOT, Département de Dermatologie, CHU de Montpellier, Montpellier; Dr Patrice CEBALLOS, Service d'Hématologie Clinique, CHU de Montpellier, Montpellier; Pr Guillaume CARTRON, Service d'Hématologie Clinique, CHU de Montpellier, Montpellier; Pr Pierre FEUGIER, Service d'Hématologie, Hôpital Brabois, Nancy; Dr Fadia DOUMAT-BATCH, Service de Dermatologie et Allergologie , CHU Nancy, Nancy; Dr Charlotte PAUGAM, Service de Dermatologie , CHU de Nantes, Nantes; Dr Jacques DANTAL, Service de Néphrologie et immunologie clinique, CHU de Nantes, Nantes; Dr Margot ROBLES, Service d'Hématologie-Oncologie, CHU de Périgueux, Périgueux; Dr Sara BURCHERI, Service d'Hématologie clinique, Centre hospitalier Saint Jean, Perpignan; Dr Antoine THIERRY, Service de néphrologie-hémodialyse et transplantation rénale., CHU de Poitiers, Poitiers; Dr Eric DUROT, Service d'Hématologie Clinique, Hôpital Robert Debré, Reims; Pr Alain DUPUY, Service de Dermatologie , CHU de Rennes, Rennes; Dr Roch HOUOT, Service d'Hématologie Clinique, CHU de Rennes, Rennes; Dr Romain CROCHETTE, Service de Néphrologie, CHU de Rennes, Rennes; Dr Anne-Bénedicte DUVAL MODESTE, Service de Dermatologie , Hôpital Charles-Nicolle, Rouen ; Dr Stéphane LEPRETRE, Service d'Hématologie, Centre Henri Becquerel, Rouen ; Dr Jérome CORNILLON, Service d'Hématologie, Institut de Cancérologie Lucien Neuwirth, Saint-Priest-en-Jarez ; Dr Elise TOUSSAINT , Service d'Hématologie, Hôpital de Hautepierre, Strasbourg; Dr Luc-Mathieu FORNECKER,

Service d'Hématologie, Hôpital de Hautepierre, Strasbourg; Pr Sophie CAILLARD, Service de Néphrologie et transplantation, CHU de Strasbourg, Strasbourg; Dr Nassim KAMAR, Service de Néphrologie et transplantation d'organes, Hôpital Rangueil, Toulouse; Dr Loic YSEBAERT , Service d'Hématologie, CHU de Toulouse, Toulouse; Pr Laurent MACHET, Service de Dermatologie , Hôpital Trousseau, Tours; Dr Caroline DARTIGEAS, Service d'Hématologie et Thérapie Cellulaire (HTC) adulte et pédiatrique, Hôpital Bretonneau, Tours, France.

FIGURE LEGENDS

Figure 1. Flow chart of the study.

Figure 2. Lymphocyte subpopulations and progression-free survival of EBV-positive and EBV-negative PTLD patients. (A) Individual measures of absolute lymphocytes counts ($CD45^+$) by group. (B-C) Kaplan Meyer curves of progression-free survival after EBV-negative and EBV-positive PTLD diagnosis according to upper (colored lines) and lower (black lines) median absolute lymphocyte counts. (D) Individual measures of absolute $CD4^+$ T-cell counts by group. (E-F) Kaplan Meyer curves of progression-free survival after EBV-negative and EBV-positive PTLD diagnosis according to upper (colored lines) and lower (black lines) median counts of $CD4^+$T cells. (G) Individual measures of absolute counts of NK ($CD3^-$ $CD56^+$/$CD16^+$) cells by group. (H-I) Kaplan Meyer curves of progression-free survival after EBV-negative and EBV-positive PTLD diagnosis according to upper (colored lines) and lower (black lines) median NK cell counts. Absolute counts of total $CD45^+$ and lymphocyte subpopulations were measured in whole fresh blood of 15 Transplant controls (TC), 55 EBV-positive and 38 EBV-negative PTLD patients Median counts were determined from the 108 individual measures among the 3 groups of patients. Differences in survival were calculated with the Log-rank test followed by false discovery rate correction (FDR=0.05). Horizontal lines in dot-plots represent medians. Median values were compared between groups with a Kruskall Wallis test and Dunn's multiple comparison post-test. Individual measures are represented as blue squares

(■) for TCs, green circles (●) for EBV-pos PTLDs and orange triangles (▲) for EBV-neg PTLDs. Only adjusted p-values are shown.

Figure 3. NK-cell activation and functionality in EBV-positive and EBV-negative PTLD patients compared to Transplant Controls. $CD3^{-}CD56^{+}$ NK cells were gated out from live lymphocytes from 11 Transplant controls , 20 EBV-positive and 18 EBV-negative PTLD patients. (A-B) Mean fluorescence intensity (MFI) of (A) CD69 and HLA-DR activation markers and (B) PD1 and TIM-3 immune-checkpoints were measured at the surface of total NK cells. (C) Spearman correlation between PD-1 expression (MFI) and EBV load in Log of International Units (IU)/mL from EBV-pos (upper panel) and EBV-neg PTLD patients (lower panel). (D) FAS cell surface death receptor (FAS) and the active form of caspase-3 were measured in total NK cells; upper panels show a representative patient of TC (blue, left); EBV-pos (green, center) and EBV-neg (orange, right) groups. Lower panels show the frequency of active caspase-3^{+} (left), FAS^{+} (center) and active caspase-3^{+} FAS^{+} (right) NK cells from patients. (H) Functional NK cells were detected by their cytokine (IFNγ) production after IL-12/IL-18 stimulation and degranulation capacity (externalization of CD107a) after incubation with K562 targets at 1:1 ratio in 5 TC, 5 EBV-pos and 6 EBV-neg PTLD patients. The frequencies of $IFN\gamma^{+}$ and $CD107a^{+}$ NK cells were compared between patients from all groups according to median NK cell counts at inclusion (median from 108 measures=90 NK cells/mm^3), whereas <90 NK cells/mm^3 were consider low counts (n=6) and >90 NK cells/mm^3 were considered normal (n=9). (I) Spearman correlation between the frequency of $IFN\gamma^{+}$ NK cells and EBV load in Log of International Units (IU)/mL in 13 patients. (J) PD1 MFI at the surface of $IFN\gamma^{+}$ NK cells by group. Lines in dot plots represent median values. Median values were compared between groups with a Kruskall Wallis test and Dunn's multiple comparison post-test. Correlations were assessed with the Spearman rank correlation coefficient. Individual measures are represented as blue squares (■) for TCs, green circles (●) for EBV-positive PTLDs and orange triangles (▲) for EBV-negative PTLDs. Only adjusted p-values are shown.

Figure 4. Activation and exhaustion phenotypes of CD4$^+$ and CD8$^+$ T cell subsets in Transplant Controls, EBV-positive and EBV-negative PTLD patients. (A) The proportion of HLA-DR$^+$ CD4$^+$ T cells was measured by flow cytometry in whole blood of 15 TC, 18 EBV-pos and 17 EBV-neg PTLD patients. (B-D) The proportions of PD-1$^+$, TIM-3$^+$ and PD-1$^+$ TIM-3$^+$ populations in CD4$^+$ T cells were determined by multiparametric flow cytometry in thawed PBMCs of of 15 TC, 42 EBV-pos and 36 EBV-neg PTLD patients.(E-F) Kaplan Meyer curves of progression-free survival after (E) EBV-neg PTLD and (F) EBV-pos PTLD diagnosis according to upper (colored lines) and lower (black lines) median frequencies of peripheral TIM-3$^+$ CD4$^+$ T cells. Medians were determined from the 93 individual measures within the 3 groups of patients. Differences in progression-free survival were calculated with the Log-rank test followed by false discovery rate correction (FDR=0.05). (G-J) The frequencies of CD38$^+$HLA-DR$^+$, PD-1$^+$, TIM-3$^+$ and PD-1$^+$ TIM-3$^+$ populations in CD8$^+$ T cells were determined as mentioned above for CD4$^+$ T cells. Horizontal lines in dot-plots represent medians. Median values were compared between groups with a Kruskall Wallis test and Dunn's multiple comparison post-test; Individual measures are represented as blue squares (■) for TCs, green circles (●) for EBV-positive PTLDs and orange triangles (▲) for EBV-negative PTLDs. Only adjusted p-values are shown.

Figure 5. EBV-specific T cell responses of patients in EBV-positive and EBV-negative PTLD patients and Transplant Controls. EBV-specific CD8$^+$ T cells were detected by intracellular cytokine staining (IFNγ or IL-2 or TNFα) with flow cytometry after after 6-hour stimulation of patients PBMCs with EBV peptides: 47 fifteen-mers covering BZLF-1 protein and 33 class II or 42 class I MHC restricted EBV epitopes. An OR boolean gate was created from IFNγ+ or IL-2+, or TNFα+ cells, within live CD3$^+$ CD8$^+$ lymphocytes (A) Frequency of total (latent + lytic) EBV-specific CD8$^+$ T cells of 15 TC, 11 EBV-pos and 16 EBV-neg PTLD patients. (B) The frequency of PD-1$^+$ and PD-1$^+$TIM-3$^+$ EBV-specific CD8$^+$ T cells was measured for 14 TC, 9 EBV-pos and 14 EBV-neg PTLD patients. Median values were compared between groups with a Kruskall Wallis test and Dunn's multiple comparison post-test. Only adjusted p-values are shown. Individual measures are represented as blue squares (■) for TCs, green circles (●) for EBV-positive PTLDs and orange triangles (▲) for EBV-negative PTLDs.

(C) Number of T cell responses detected with ELISpot-IFNγ against EBV peptides (from top to bottom): 33 class II-MHC restricted peptides divided in 3 pools; 42 class I-MHC restricted peptides divided in 5 pools and 47 and 160 fifteen-mers covering BZLF-1 (5 pools) and EBNA-3A (16 pools) proteins. Individual responses were measured in triplicate assays after background subtraction; each bar represents the number of individual responses against each peptide pool. The number of responders by group against EBNA-3A pools 1 to 4, which include EBNA-3 homology region (gray background) were compared by X^2 test. *P<0.05. (H) Relative contribution of BZLF-1 (light) and EBNA-3A (dark) responses= (BZLF-1 x 100)|/|(BZLF-1+EBNA-3A), data of each tested patient is shown, numbers in the y axis correspond to individual ID by group, while numbers in the x axis indicate proportions.

Figure 6. PD-L1 expression and T-cell infiltration of EBV-positive and EBV-negative PTLD tumors. Representative images of tumor biopsies from one EBV-positive PTLD (left) and one EBV-negative PTLD (right) following cardiac transplantation. (A-B) EBV status of the tumor was determined by EBER in-situ hybridization (light microscopy, original magnification X200). (C-D) Hematoxylin-Eosin-Safran staining (HES; light microscopy, original magnification X400) showing cellular infiltration in sections of (C) EBER+ plasmablastic lymphoma (colon) and (D) EBER- diffuse large B-cell lymphoma (liver). (E-J) Immunohistochemistry for the indicated markers (light microscopy, original magnification X200). PD-L1 expression by tumor cells was broader in the (E) EBV-positive PTLD (90%) than in the (F) EBV-negative PTLD (30%), while low $CD3^+$ T-cell infiltration is observed in both (G) EBV-positive and (H) EBV-negtive tumors; note that T cells represent 10% of cellular infiltrate in both cases, with similar ratios between T cells and tumor cells; while $CD8^+$ T-cell infiltration represents 80% of T cells in the (I) EBV-positive tumor but only 30% in the (J) EBV-negative tumor. Immunostaining was performed on formalin fixed, deparaffinized sections by using Ventana Benchmark Ultra platform and the Optiview visualization system.

Figure 7. Immunopathology model of EBV-positive and EBV-negative PTLD. A model is proposed based on the experimental findings of the present study and previous published results.[14] (A) Life-long EBV infection in healthy immunocompetent individuals is maintained under control by T and NK cell immunosurveillance. (B) In transplant recipients, such immunosurveillance is weakened by therapeutic immunosuppression, to the benefit of EBV reactivation or primo-infection. Close to transplantation $CD4^+$ T cell lymphopenia is common but might persist to the long term, involving a specific loss of Th1 EBV-specific $CD4^+$ T cells. In parallel, intense stimuli from viral and graft allo-antigens promote activation of $CD8^+$ T cell effectors and might as well favor PD-1 upregulation in both $CD8^+$ T and NK cytotoxic lymphocytes. (C) The majority of EBV-positive PTLDs occur during that critical period of intense immunosuppression. Such early incidence is probably related with the survival advantages provided by viral proteins to EBV-infected tumor-cells, which fast proliferation can no longer be contained by the low number of circulating NK and EBV-specific $CD8^+$ T cells. NK cells are highly activated (HLA-DR), overexpress PD-1 and might be depleted from periphery due to high activation-induced cell death, while Th1 responses against latent EBV are low. and $CD8^+$ T-cell responses poorly recognize the N-terminal portion of the viral protein EBNA-3A. In addition, peripheral EBV-specific $CD8^+$ T cells are exhausted (PD-1/TIM-3). The tumor microenvironment presents $CD8^+$ T-cell infiltration which may be exhausted meeting their PD-1 ligand expressed by tumor cells. Thus, early development of EBV-positive PTLD might be accelerated in SOT recipients undergoing primary EBV-infection, who present higher NK-cell activation possibly leading to increased AICD, while the establishment primary CD8+T cell responses lack proper Th1 help. (D) Nonetheless, almost half of PTLDs arise several years after transplantation, without association to EBV. Those EBV-negative PTLD patients might carry detectable EBV loads but share similar EBV-specific T cell responses than PTLD-free transplant recipients. In contrast, $CD4^+$ T cell lymphopenia, particularly when accompanied of a high proportion of $TIM\text{-}3^+$ $CD4^+$ T cells in peripheral blood, is associated with poor outcomes. In addition, of NK cells overexpress TIM-3 immune-checkpoint too. Thus, Tim-3 might either contribute to or be a consequence of a drastic acceleration of the disease. In addition, T cell infiltrate in the tumor is low.

SUPPORTING INFORMATION STATEMENT

Additional supporting information may be found online in the Supporting Information section at the end of the article.

REFERENCES

1. Dierickx D, Habermann TM. Post-Transplantation Lymphoproliferative Disorders in Adults. Longo DL, ed. *N Engl J Med*. 2018;378(6):549-562. doi:10.1056/NEJMra1702693
2. Dharnidharka VR, Webster AC, Martinez OM, Preiksaitis JK, Leblond V, Choquet S. Post-transplant lymphoproliferative disorders. *Nat Rev Dis Prim*. 2016;2(1):15088. doi:10.1038/nrdp.2015.88
3. Luskin MR, Heil DS, Tan KS, et al. The Impact of EBV Status on Characteristics and Outcomes of Posttransplantation Lymphoproliferative Disorder. *Am J Transplant*. 2015;15(10):2665-2673. doi:10.1111/ajt.13324
4. Martinez OM, Krams SM. The Immune Response to Epstein Barr Virus and Implications for Posttransplant Lymphoproliferative Disorder. *Transplantation*. 2017;101(9):2009-2016. doi:10.1097/TP.0000000000001767
5. Leblond V, Davi F, Charlotte F, et al. Posttransplant lymphoproliferative disorders not associated with Epstein-Barr virus: a distinct entity? *J Clin Oncol*. 1998;16(6):2052-2059. doi:10.1200/JCO.1998.16.6.2052
6. Baychelier F, Achour A, Nguyen S, et al. Natural killer cell deficiency in patients with non-Hodgkin lymphoma after lung transplantation. *J Hear Lung Transplant*. 2015;34(4):604-612. doi:10.1016/j.healun.2014.09.038
7. Wiesmayr S, Webber SA, Macedo C, et al. Decreased NKp46 and NKG2D and elevated PD-1 are associated with altered NK-cell function in pediatric transplant patients with PTLD. *Eur J Immunol*. 2012;42(2):541-550. doi:10.1002/eji.201141832
8. Jones K, Nourse JP, Morrison L, et al. Expansion of EBNA1-specific effector T cells in posttransplantation lymphoproliferative disorders. *Blood*. 2010;116(13):2245-2252. doi:10.1182/blood-2010-03-274076
9. Wilsdorf N, Eiz-Vesper B, Henke-Gendo C, et al. EBV-specific T-Cell immunity in pediatric solid organ graft recipients with posttransplantation lymphoproliferative disease. *Transplantation*. 2013;95(1):247-255. doi:10.1097/TP.0b013e318279968d
10. Ning RJ, Xu XQ, Chan KH, Chiang AKS. Long-term carriers generate Epstein-Barr virus (EBV)-specific CD4+and CD8+polyfunctional T-cell responses which show immunodominance hierarchies of EBV proteins. *Immunology*. 2011;134(2):161-171. doi:10.1111/j.1365-2567.2011.03476.x

11. Moran J, Dean J, De Oliveira A, et al. Increased levels of PD-1 expression on CD8 T cells in patients post-renal transplant irrespective of chronic high EBV viral load. *Pediatr Transplant*. 2013;17:806-814. doi:10.1111/petr.12156

12. Ma S-D, Xu X, Jones R, et al. PD-1/CTLA-4 Blockade Inhibits Epstein-Barr Virus-Induced Lymphoma Growth in a Cord Blood Humanized-Mouse Model. Ling PD, ed. *PLOS Pathog*. 2016;12(5):e1005642. doi:10.1371/journal.ppat.1005642

13. Macedo C, Webber S a, Donnenberg AD, et al. EBV-specific CD8+ T cells from asymptomatic pediatric thoracic transplant patients carrying chronic high EBV loads display contrasting features: activated phenotype and exhausted function. *J Immunol*. 2011;186(10):5854-5862. doi:10.4049/jimmunol.1001024

14. Nakid-Cordero C, Arzouk N, Gauthier N, et al. Skewed T cell responses to Epstein-Barr virus in long-term asymptomatic kidney transplant recipients. Drummond J, ed. *PLoS One*. 2019;14(10):e0224211. doi:10.1371/journal.pone.0224211

15. Rea D, Fourcade C, Leblond V, et al. Patterns of Epstein-Barr virus latent and replicative gene expression in Epstein-Barr virus B cell lymphoproliferative disorders after organ transplantation. *Transplantation*. 1994;58(3):317-324. doi:0041-1337/94

16. Gratama JW, Zutter MM, Minarovits J, et al. Expression of epstein-barr virus-encoded growth-transformation-associated proteins in lymphoproliferations of bone-marrow transplant recipients. *Int J Cancer*. 1991;47(2):188-192. doi:10.1002/ijc.2910470205

17. Fink SEK, Gandhi MK, Nourse JP, et al. A comprehensive analysis of the cellular and EBV-specific microRNAome in primary CNS PTLD identifies different patterns among EBV-associated tumors. *Am J Transplant*. 2014;14(11):2577-2587. doi:10.1111/ajt.12858

18. Calarota SA, Chiesa A, Zelini P, Comolli G, Minoli L, Baldanti F. Detection of Epstein-Barr virus-specific memory CD4+ T cells using a peptide-based cultured enzyme-linked immunospot assay. *Immunology*. 2013;139(4):533-544. doi:10.1111/imm.12106

19. Haque T, Wilkie GM, Jones MM, et al. Allogeneic cytotoxic T-cell therapy for EBV-positive posttransplantation lymphoproliferative disease: Results of a phase 2 multicenter clinical trial. *Blood*. 2007;110(4):1123-1131. doi:10.1182/blood-2006-12-063008

20. Bieling M, Tischer S, Kalinke U, et al. Personalized adoptive immunotherapy for patients with EBV-associated tumors and complications: Evaluation of novel naturally processed and presented EBV-derived T-cell epitopes. *Oncotarget*. 2018;9(4):4737-4757. doi:10.18632/oncotarget.23531

21. Bollard CM, Heslop HE. ADVANCES IN CELL-BASED IMMUNE THERAPEUTICS IN HEMATOLOGY T cells for viral infections after allogeneic hematopoietic stem cell transplant. 2016;127(26):3331-3341. doi:10.1182/blood-2016-01-628982.

22. Gallot G, Vollant S, Saïagh S, et al. T-cell therapy using a bank of EBV-specific Cytotoxic T cells: Lessons from a phase I/II feasibility and safety study. *J Immunother*. 2014;37(3):170-179. doi:10.1097/CJI.0000000000000031

23. Choquet S, Varnous S, Deback C, Golmard JL, Leblond V. Adapted treatment

of epstein-barr virus infection to prevent posttransplant lymphoproliferative disorder after heart transplantation. *Am J Transplant*. 2014;14(4):857-866. doi:10.1111/ajt.12640

24. Achour A, Baychelier F, Besson C, et al. Expansion of CMV-mediated NKG2C+ NK cells associates with the development of specific de novo malignancies in liver-transplanted patients. *J Immunol*. 2014;192(1):503-511. doi:10.4049/jimmunol.1301951
25. Peraldi MN, Berrou J, Venot M, et al. Natural killer lymphocytes are dysfunctional in kidney transplant recipients on diagnosis of cancer. *Transplantation*. 2015;99(11):2422-2430. doi:10.1097/TP.0000000000000792
26. Bennabi M, Tarantino N, Gaman A, et al. Persistence of dysfunctional natural killer cells in adults with high-functioning autism spectrum disorders: Stigma/consequence of unresolved early infectious events? *Mol Autism*. 2019;10(1):1-13. doi:10.1186/s13229-019-0269-1
27. Trappe RU, Choquet S, Dierickx D, et al. International prognostic index, type of transplant and response to rituximab are key parameters to tailor treatment in adults with cd20-positive b cell ptld: Clues from the ptld-1 trial. *Am J Transplant*. 2015;15(4):1091-1100. doi:10.1111/ajt.13086
28. Kinch A, Baecklund E, Backlin C, et al. A population-based study of 135 lymphomas after solid organ transplantation: The role of Epstein-Barr virus, hepatitis C and diffuse large B-cell lymphoma subtype in clinical presentation and survival. *Acta Oncol (Madr)*. 2014;53(5):669-679. doi:10.3109/0284186X.2013.844853
29. Caillard S, Porcher R, Provot F, et al. Post-transplantation lymphoproliferative disorder after kidney transplantation: Report of a nationwide French registry and the development of a new prognostic score. *J Clin Oncol*. 2013;31(10):1302-1309. doi:10.1200/JCO.2012.43.2344
30. Walti LN, Mugglin C, Sidler D, et al. Association of antiviral prophylaxis and rituximab use with posttransplant lymphoproliferative disorders (PTLDs): A nationwide cohort study. *Am J Transplant*. 2020. doi:10.1111/ajt.16423
31. Galluzzi L, Vitale I, Aaronson SA, et al. Molecular mechanisms of cell death: Recommendations of the Nomenclature Committee on Cell Death 2018. *Cell Death Differ*. 2018;25(3):486-541. doi:10.1038/s41418-017-0012-4
32. Crowley LC, Waterhouse NJ. Detecting cleaved caspase-3 in apoptotic cells by flow cytometry. *Cold Spring Harb Protoc*. 2016;2016(11):958-962. doi:10.1101/pdb.prot087312
33. Zimmermann H, Choquet S, Moore J, et al. Baseline differential blood count and prognosis in CD20-positive post-transplant lymphoproliferative disorder in the prospective PTLD-1 trial. *Leukemia*. 2013;27(10):2102-2105. doi:10.1038/leu.2013.110
34. Styles C, Paschos K, White R, Farrell P. The Cooperative Functions of the EBNA3 Proteins Are Central to EBV Persistence and Latency. *Pathogens*. 2018;7(1):31. doi:10.3390/pathogens7010031
35. Quinlan SC, Pfeiffer RM, Morton LM, Engels EA. Risk factors for early-onset and late-onset post-transplant lymphoproliferative disorder in kidney recipients in the United States. *Am J Hematol*. 2011;86(2):206-209. doi:10.1002/ajh.21911

36. Dharnidharka VR. Comprehensive review of post–organ transplant hematologic cancers. *Am J Transplant*. 2018;18(3):537-549. doi:10.1111/ajt.14603

37. Morscio J, Dierickx D, Ferreiro JF, et al. Gene Expression Profiling Reveals Clear Differences Between EBV-Positive and EBV-Negative Posttransplant Lymphoproliferative Disorders. *Am J Transplant*. 2013;13(5):1305-1316. doi:10.1111/ajt.12196

38. Menter T, Juskevicius D, Alikian M, et al. Mutational landscape of B-cell post-transplant lymphoproliferative disorders. *Br J Haematol*. 2017;178(1):48-56. doi:10.1111/bjh.14633

39. Naik S, Riches M, Hari P, et al. Survival outcomes of allogeneic hematopoietic cell transplants with EBV-positive or EBV-negative post-transplant lymphoproliferative disorder, A CIBMTR study. *Transpl Infect Dis*. 2019;(January):1-10. doi:10.1111/tid.13145

40. Watanabe M, Kanda J, Hishizawa M, et al. Lymphopenia at diagnosis predicts survival of patients with immunodeficiency-associated lymphoproliferative disorders. *Ann Hematol*. 2020;99(7):1565-1573. doi:10.1007/s00277-020-04084-5

41. Ménétrier-Caux C, Ray-Coquard I, Blay JY, Caux C. Lymphopenia in Cancer Patients and its Effects on Response to Immunotherapy: An opportunity for combination with Cytokines? *J Immunother Cancer*. 2019;7(1):1-15. doi:10.1186/s40425-019-0549-5

42. Yang Z-Z, Grote DM, Ziesmer SC, et al. IL-12 upregulates TIM-3 expression and induces T cell exhaustion in patients with follicular B cell non-Hodgkin lymphoma. *J Clin Invest*. 2012;122(4):1271-1282. doi:10.1172/JCI59806

43. Monabati A, Vahedi A, Safaei A, et al. Epstein-Barr Virus-Positive Diffuse Large B-Cell Lymphoma: is it different between Over and Under 50 Years of Age? *Asian Pacific J Cancer Prev*. 2016;17(4):2285-2289. doi:10.7314/APJCP.2016.17.4.2285

44. Ndhlovu LC, Lopez-verge S, Barbour JD, et al. Tim-3 marks human natural killer cell maturation and suppresses cell-mediated cytotoxicity. *Blood*. 2012;119(16):3734-3743. doi:10.1182/blood-2011-11-392951.

45. Gonçalves Silva I, Yasinska IM, Sakhnevych SS, et al. The Tim-3-galectin-9 Secretory Pathway is Involved in the Immune Escape of Human Acute Myeloid Leukemia Cells. *EBioMedicine*. 2017;22:44-57. doi:10.1016/j.ebiom.2017.07.018

46. Tallerico R, Cristiani CM, Staaf E, et al. IL-15, TIM-3 and NK cells subsets predict responsiveness to anti-CTLA-4 treatment in melanoma patients. *Oncoimmunology*. 2017;6(2):e1261242. doi:10.1080/2162402X.2016.1261242

47. Hadadi L, Hafezi M, Amirzargar AA, Sharifian RA, Abediankenari S, Asgarian-Omran H. Dysregulated Expression of Tim-3 and NKp30 Receptors on NK Cells of Patients with Chronic Lymphocytic Leukemia. *Oncol Res Treat*. 2019;42(4):197-203. doi:10.1159/000497208

48. So EC, Khaladj-Ghom A, Ji Y, et al. NK cell expression of Tim-3: First impressions matter. *Immunobiology*. 2019;224(3):362-370. doi:10.1016/j.imbio.2019.03.001

49. Xu L, Huang Y, Tan L, et al. Increased Tim-3 expression in peripheral NK cells

predicts a poorer prognosis and Tim-3 blockade improves NK cell-mediated cytotoxicity in human lung adenocarcinoma. *Int Immunopharmacol*. 2015;29(2):635-641. doi:10.1016/j.intimp.2015.09.017

50. Bachanova V, Sarhan D, DeFor TE, et al. Haploidentical natural killer cells induce remissions in non-Hodgkin lymphoma patients with low levels of immune-suppressor cells. *Cancer Immunol Immunother*. 2018;67(3):483-494. doi:10.1007/s00262-017-2100-1

51. Liu E, Marin D, Banerjee P, et al. Use of CAR-transduced natural killer cells in CD19-positive lymphoid tumors. *N Engl J Med*. 2020;382(6):545-553. doi:10.1056/NEJMoa1910607

52. Markasz L, Vanherberghen B, Flaberg E, et al. NK cell-mediated lysis is essential to kill Epstein-Barr virus transformed lymphoblastoid B cells when using rituximab. *Biomed Pharmacother*. 2009;63(6):413-420. doi:10.1016/j.biopha.2008.08.009

53. Guihot A, Dupin N, Marcelin A-G, et al. Low T cell responses to human herpesvirus 8 in patients with AIDS-related and classic Kaposi sarcoma. *J Infect Dis*. 2006;194(8):1078-1088. doi:JID36629 [pii]\r10.1086/507648

54. Dugan JP, Haverkos BM, Villagomez L, et al. Complete and Durable Responses in Primary Central Nervous System Posttransplant Lymphoproliferative Disorder with Zidovudine, Ganciclovir, Rituximab, and Dexamethasone. *Clin Cancer Res*. 2018;24(14):3273-3281. doi:10.1158/1078-0432.CCR-17-2685

55. Kroll J, Li S, Levi M, Weinberg A. Lytic and latent EBV gene expression in transplant recipients with and without post-transplant lymphoproliferative disorder. *J Clin Virol*. 2011;52(3):231-235. doi:10.1016/j.jcv.2011.06.013

56. Green MR, Rodig S, Juszczynski P, et al. Constitutive AP-1 activity and EBV infection induce PD-l1 in Hodgkin lymphomas and posttransplant lymphoproliferative disorders: Implications for targeted therapy. *Clin Cancer Res*. 2012;18(6):1611-1618. doi:10.1158/1078-0432.CCR-11-1942

57. Kinch A, Sundström C, Baecklund E, Backlin C, Molin D, Enblad G. Expression of PD-1, PD-L1, and PD-L2 in posttransplant lymphoproliferative disorder after solid organ transplantation. *Leuk Lymphoma*. 2018;0(919):1-9. doi:10.1080/10428194.2018.1480767

58. Apetoh L, Smyth MJ, Drake CG, et al. Consensus nomenclature for CD8+ T cell phenotypes in cancer. *Oncoimmunology*. 2015;4(4):1-10. doi:10.1080/2162402X.2014.998538

59. O'Reilly RJ, Prockop S, Hasan AN, Koehne G, Doubrovina E. Virus-specific T-cell banks for "off the shelf" adoptive therapy of refractory infections. *Bone Marrow Transplant*. 2016;51(9):1163-1172. doi:10.1038/bmt.2016.17

60. Dasari V, Bhatt KH, Smith C, Khanna R. Designing an effective vaccine to prevent Epstein-Barr virus-associated diseases: challenges and opportunities. *Expert Rev Vaccines*. 2017;16(4):377-390. doi:10.1080/14760584.2017.1293529

61. de Bruijn S, Anguille S, Verlooy J, et al. Dendritic Cell-Based and Other Vaccination Strategies for Pediatric Cancer. *Cancers (Basel)*. 2019;11(9):1396. doi:10.3390/cancers11091396

Table 1. Patients characteristics

	TC n=21	EBV-pos PTLD n=56	EBV-neg PTLD n=39	*P* *
Sex , n (%)				
Male	16 (76%)	35 (63%)	26 (67%)	0.6763
Female	5 (24%)	21 (37%)	13 (33%)	
Age at transplantation, median (min-max)	46 (21-71)	52 (19-73)	51 (14-72)	0.7047
Transplant Type, n (%)				
Renal	10 (48%)	37 (66%)	20 (51%)	
Hepatic	10 (48%)	9 (16%)	11 (28%)	
Cardiac		7 (13%)	5 (13%)	
Pulmonary		3 (5%)	1 (3%)	
Multiple	1 (4%) †		2 (5%) ‡	
IS regimen, n (%)				
Glucocorticoids	16 (76%)	44 (79%)	22 (56%)	0.1940
Antimetabolites	15 (71%)	40 (71%)	22 (56%)	0.4865
Calcineurin Inhibitors	17 (81%)	42 (75%)	33 (85%)	0.6763
mTOR inhibitors	3 (14%)	8 (14%)	4 (10%)	0.8297
EBV pre-transplant serology, n (%)				
Positive	13 (62%)	25 (45%)	23 (59%)	
Negative	1 (5%)	9 (16%)	1 (3%)	
Unknown	7 (33%)	22 (39%)	15 (38%)	
Re-transplantation before inclusion	1 (5%)	0 (0%)	4 (10%)	
EBV load at PTLD diagnosis Log of UI/mL, median (min-max)	2.1 (1.6-3.8)	3.7 (1.6-5.7)	2.6 (1.6-5.4)	0.0009#
Time from last transplant to PTLD, years, median (min-max)	8 (2-37)	7.5 (1-27)	10 (1-42)	0.1940
PTLD occurrence, § n (%)				
Early (≤4 years after transplantation)		22 (39%)	8 (21%)	0.1940
Late (>4 years after transplantation)		34 (61%)	31 (79%)	
Lymphoma histopathology, n (%)				
Early lesions				
Lymphoblastocytic infiltrate		1 (2%)		
Polymorphic PTLD		8 (14%)		
Monomorphic PTLD				
DLBCL		32 (57%)	28 (72%)	
Follicular lymphoma		1 (2%)		
Marginal zone lymphoma			5 (13%)	
Plasmablastic lymphoma		4 (7%)		
Plasmacytoma			2 (5%)	
B-cell lymphoma		7 (13%)		
T cell lymphoma			2 (5%)	
Burkitt lymphoma			2 (5%)	
Classical Hodgkin lymphoma		3 (5%)		
PTLD localization, n (%)				
Lymph nodes only		7 (13%)	12 (31%)	

Allograft		2 (4%)	3 (8%)	
Bone marrow		0 (0%)	4 (10%)	
CNS		29 (52%)	1 (2%)	
Liver		6 (11%)	6 (15%)	
Lung/Pleura		4 (7%)	5 (13%)	
Gi Tract		8 (14%)	10 (26%)	
Other		3 (5%)	6 (15%)	
Suvival, ‖ n				
Alive	15	34	23	
Dead		17	15	
Unknown	6	5	1	

*Statistical differences between groups were assessed with Chi-square test or Kruskal-Wallis test followed by false discovery rate correction (FDR=0.05). Only multiplicity adjusted P-values are shown.

† Multiple renal and cardiac transplantation.

‡ Multiple pulmonary and renal or renal and hepatic transplantation.

Differences between groups were determined with Dunn's post-test. TC vs EBV-pos P=0.0021; EBV-neg vs EBV-pos P=0.0015.

§ PTLD onset was considered early 0-4 years after transplantation and late over 4 years after transplantation.

|| Last survival checkpoint was between February 2019 and January 2020.

Supplemental data

Supplemental Methods

Transplant controls inclusion criteria

Inclusion criteria for all transplant controls were: age >18 years old at inclusion, no history of acute graft rejection, malignancy or recurrent infections at least two years before inclusion. We selected patients with different post- transplant delays to match both early and late PTLD patients.

Blood Samples

Blood samples from patients and controls were collected at inclusion during consultation in 5 mL tubes containing Ethylenediaminetetraacetic acid (EDTA) or Lithium heparin. All samples were centralized and immediately processed at the Department of Immunology of the Pitié-Salpêtrière Hospital. Samples from controls belonging to the K-GREF cohort had been previously collected under the same conditions and were already available in our cell-bank the Department of Immunology. Absolute T/B/NK lymphocyte counts and T-cell phenotype were measured on fresh EDTA-collected blood as previously described:[1]

Absolute lymphocyte counts

Total and T/B/NK lymphocyte absolute counts were determined with an automated AQUIOS CL flow cytometry system (Beckman Coulter, Villepinte, France) using

commercial kits AQUIOS Tetra-1 Panel (ref: B23533) and Tetra-2+ Panel (B23534) according to manufacturer's instructions (Beckman Coulter).

T cell differentiation and activation phenotype

T cell differentiation and activation markers were measured on EDTA-collected whole blood within the $CD45^+$ lymphocytes, gated on the $CD3^+CD4^+$ or $CD3^+CD8^+$ populations, by using following antibodies: anti-CD45-APC-A750, anti-CD8-APC-A700, anti-CD4-PB, anti-CD57-FITC, anti-CD45RA-ECD, anti-HLA DR-ECD, anti-CD25-PE, anti-CD38-Pc7 (Beckman Coulter), anti-CD3-APC, anti-CD95-FITC (BD Biosciences, Le Pont de Claix, France) and anti-CCR7-PE (Agilent Technologies, Les Ulis, France). A TQ-Prep Workstation (Beckman Coulter) was used for incubation, cell lysis and fixation of samples (IMMUNOPREP™ Reagent System, Beckman Coulter). Samples were acquired with a Navios flow cytometer (Beckman Coulter).

PBMC cryopreservation and thawing procedures

Blood collected in Lithium heparin tubes was diluted 1:2 in RPMI 1640 medium (Thermo Fisher Scientific, Villebon-sur-Yvette, Courtaboeuf, France) before 30 minutes centrifugation at 2200 revolutions per minute (rpm) through Lymphocyte separation density gradient media (Eurobio, les Ulis, Courtaboeuf, France). The ring containing the peripheral blood mononuclear cells (PBMC) was recovered, washed twice with RPMI 1640 medium for 8 minutes at 1700rpm, then suspended in 10% Dimethyl Sulfoxide (DMSO, Sigma-Aldrich, Missouri, USA) heat-inactivated Fetal

Bovine Serum (FBS, Biowest, Nuaillé, France). Samples from all patients and controls were cryopreserved in liquid nitrogen cell bank at the Department of Immunology of the Pitié-Salpêtrière Hospital until use.

PBMCs were thawed in RPMI+ medium (100 UI/mL penicillin / 100 µg/mL streptomycin / 0.25 µg/mL Amphotericin B, 1 mM sodium pyruvate, 0.1 mM MEM NEAA, 2mM L-glutamine; Thermo Fisher Scientific) supplemented with 20% FBS (Biowest), then washed twice with RPMI+ medium 10% FBS and suspended in proper media for each specific test.

NK cell phenotype and functional assays

Thawed PBMCs were stained with Fixable viability Dye-Efluor 506 (Invitrogen, Courtaboeuf, France), anti-CD16-PerCP-Cy5.5, anti-NKp30-BV421, anti-PD1-PE, anti-TIM-3-BV421, anti CD95-APC, (BD Biosciences), anti-CD69-ECD, anti-NKG2A-PE, anti-CD56-PC7, Kir2DL2/DL3-PE, anti-CD57-PB (Beckman coulter), anti-Kir3DL1-AF700, anti-HLA-DR-AF700 (BioLegend, CA, USA), anti-CD3-E-Fluor780 (eBioscience, Courtaboeuf, France), anti-NKp46-ECD, anti-CD16-PerCP-Vio700 (Miltenyi Biotec, Paris, France), and anti-NKG2C-APC (RD systems, Lille, France). The anti-active caspase-3-FITC and anti-IFNγ-AF700 (Becton Dickinson) were added after cell-permeabilization (Cytofix/Cytoperm™ kit; BD Biosciences).

T- cell exhaustion phenotype and functional assays

Immune-checkpoints (PD-1 and TIM-3) expression was assessed in thawed PBMCs stained with: viability stain 700-APC-R700, anti-CD8-PerCP-Cy5.5, anti-CD4-APC, anti-CD3-APC-H7, anti-PD-1-BV421 and anti-TIM-3-BV711 (BD Biosciences). For

EBV-specific T cell detection, cells were stained with viability stain 700-APC-R700, anti-PD-1-BV421 and anti-TIM-3-BV711 (BD Biosciences). After permeabilization (FIX&PERM®, ThermoFisher Scientific, Courtaboeuf, France), anti-CD8-PerCP-Cy5.5, anti-CD4-APC, anti-CD3-APC-H7, anti-IFNγ-FITC, anti-IL-2-PE-CF594, and anti-TNFα-PE-Cy7 were added (BD Biosciences). Samples were acquired with a LSR Fortessa (BD Biosciences) at the Flow Cytometry Core CyPS (Sorbonne University, Pitié-Salpêtrière Hospital).

ELISpot-IFNγ assays were performed as previously described[1] using Diaclone's ELISpot-IFNγ-pair-antibodies; briefly, 10^5 PBMCs/well were plated (Merck Millipore, Molsheim, France) in triplicates with medium, phytohemagglutinin (2µg/mL, Sigma-Aldrich) or EBV-peptide pools (2µg/mL). Plates were developed with Streptavidin-alkaline phosphatase conjugate (Amersham, Freiburg, Germany) and NBT/BCIP substrate (Sigma-Aldrich) then air-dried for 24 hours before Spot forming cell units (SFC) were read (AID Elispot reader, Autoimmun Diagnostika GmbH, Straßberg, Germany). Results are expressed as mean SFC $x10^6$ from triplicates after background subtraction. Positivity threshold was set at 50 SFC/10^6 PBMC.

Immunohistochemistry

The immunostaining procedure was performed on formalin fixed, deparaffinized, 3µm thick sections by using Ventana Benchmark Ultra platform (Roche Diagnostics, France) and the visualization system Optiview (Roche Diagnostics) according to manufacturer's instructions. The following primary antibodies were used: rabbit monoclonal anti-CD3 antibody (prediluted; clone 2GV6; ref. 790-4341, Roche

Diagnostics) with the following antigen retrieval (CC1, 64 min, 98°C) and antibody incubation time of 32 min at 36°C; rabbit monoclonal anti-human CD4 (prediluted; clone SP35; ref. 790-4423, Roche Diagnostics) with the following antigen retrieval (CC1, 32 min, 98°C) and antibody incubation time of 32 min at 36°C; mouse monoclonal anti-human CD8 (dilution 1:100; clone C8/144B; ref. M7103, Agilent) with the following antigen retrieval (CC1, 32 min, 98°C) and antibody incubation time of 32 min at 36°C ; rabbit monoclonal anti-human PD-L1 (prediluted; clone QR1; ref.1-PR292, Quartett Biochemicals) with the following antigen retrieval (CC1, 32 min, 98°C) and antibody incubation time of 32 min at 36°C.

EBV Peptides

EBV peptides included: previously published epitopes[2,3] matching different class I (n=42) and class II (n=33) HLA on latent and lytic EBV proteins (supplemental Table 1 and 2; GeneCust Europe, Ellange, Luxembourg), 15-mers overlapping by 10 amino acids (AA) and covering BZLF-1 (supplemental Table 3; GeneCust Europe) and EBNA-3A proteins (supplemental Table 4; Epytop, Nimes, France).[1] As shown in supplemental tables 1 to 4, all peptides were studied by ELISpot IFNγ but only HLA-restricted and BZLF-1 15-mer peptides were used for intracellular cytokine staining (ICS) due to sample availability.

Epitope-HLA binding prediction

The class-I and class-II HLA alleles from patients were obtained through the K-Virogref network when possible. BZLF-1 and EBNA-3A 9-mers and 15-mers binding to patients HLA were predicted with NetMHCpan 4.0[4] and NetMHCIIpan 3.2,[5] respectively.

Univariate and multivariate analysis

Exploratory univariate analysis were performed with cox-regression models for time-to-event outcomes. Event was defined as death for overall survival and disease progression or death for progression-free survival. Continuous variables were dichotomized using previously defined cut-off values[6] (age at PTLD diagnosis and delay from transplantation to PTLD) or median values from all available measures ($CD4^+$ T cells/mm^3 and % of TIM-3^+ $CD4^+$ T cells). Categorical variables such as PTLD localization, LDH at diagnosis and PTLD morphology were dichotomized to compare previously reported poor prognosis factors vs other (CNS vs systemic, elevated LDH vs normal LDH and monomorphic vs polymorphic disease).[6,7] Multivariate cox-regression modeled significant factors in univariate analysis.

References

1. Nakid-Cordero C, Arzouk N, Gauthier N, et al. Skewed T cell responses to Epstein-Barr virus in long-term asymptomatic kidney transplant recipients. Drummond J, ed. *PLoS One*. 2019;14(10):e0224211. doi:10.1371/journal.pone.0224211
2. Woodberry T, Suscovich TJ, Henry LM, et al. Differential Targeting and Shifts in the Immunodominance of Epstein-Barr Virus–Specific CD8 and CD4 T Cell Responses during Acute and Persistent Infection. *Evol T Cell Immun Dur EBV Infect @BULLET JID*. 2005;192(5214).
3. Rickinson AB, Moss DJ. HUMAN CYTOTOXIC T LYMPHOCYTE RESPONSES TO EPSTEIN-BARR VIRUS INFECTION. *Annu Rev Immunol*. 1997;15(1):405-431. doi:10.1146/annurev.immunol.15.1.405
4. Jurtz V, Paul S, Andreatta M, Marcatili P, Peters B, Nielsen M. NetMHCpan-4.0: Improved Peptide–MHC Class I Interaction Predictions Integrating Eluted Ligand and Peptide Binding Affinity Data. *J Immunol*. 2017;199(9):3360-3368. doi:10.4049/jimmunol.1700893
5. Jensen KK, Andreatta M, Marcatili P, et al. Improved methods for predicting peptide binding affinity to MHC class II molecules. *Immunology*. 2018;154(3):394-406. doi:10.1111/imm.12889
6. Trappe RU, Choquet S, Dierickx D, et al. International prognostic index, type of

transplant and response to rituximab are key parameters to tailor treatment in adults with cd20-positive b cell ptld: Clues from the ptld-1 trial. *Am J Transplant*. 2015;15(4):1091-1100. doi:10.1111/ajt.13086

7. Caillard S, Porcher R, Provot F, et al. Post-transplantation lymphoproliferative disorder after kidney transplantation: Report of a nationwide French registry and the development of a new prognostic score. *J Clin Oncol*. 2013;31(10):1302-1309. doi:10.1200/JCO.2012.43.2344

Supplemental Tables

Supplemental Table 1. Sequences of MHC-class I-restricted EBV epitopes used in intracellular cytokine staining (ICS) and ELISpot IFNγ assays.

42 8-11 mers MHC-class I-restricted epitopes were divided in 5 peptide pools

Protein	Epitope	HLA	Sequence	Pools for ELISpot IFNγ	ICS #Tube
EBNA-3A	246–253	A24	RYSIFFDY	1	1
EBNA-3A	603–611	A3	RLRAEAQVK	1	1
EBNA-3A	458–466	B35	YPLHEQHGM	1	1
EBNA-3A	406–414	B62	LEKARGSTY	1	1
EBNA-3A	379–387	B7	RPPIFIRRL	1	1
EBNA-3A	502–510	B7	VPAPAGPIV	1	1
EBNA-3A	325–333	B8	FLRGRAYGL	1	1
EBNA-3B	399–408	A11	AVFDRKSDAK	1	1
EBNA-3A	158–166	B8	QAKWRLQTL	2	1
EBNA-3B	416–424	A11	IVTDFSVIK	2	1
EBNA-3B	217–225	A24.02	TYSAGIVQI	2	1
EBNA-3B	657–666	B44	VEITPYKPTW	2	1
EBNA-3B	831–839	B62	GQGGSPTAM	2	1
EBNA-3C	284–293	A2.01	LLDFVRFMGV	2	1
EBNA-3C	881–889	B7	QPRAPIRPI	2	1
LMP-2	340-350	A11	SSCSSCPLSKI	2	1
LMP-2	329-337	A2.01	LLWTLVVLL	2	1
LMP-2	419-427	A24	TYGPVFMCL	2	1
EBNA-3A	596-604	A2	SVRDRLARL	3	1
EBNA-3A	491-499	A29	VFSDGRVAC	3	1
EBNA-3A	176-184	A30.02	AYSSWMYSY	3	1
EBNA-3B	244-254	B27.02	RRARSLSAERY	3	1
EBNA-3B	149-157	B27.05	HRCQAIRKK	3	1
EBNA-3B	488-496	B35	AVLLHEESM	3	1
EBNA-3C	258-266	B27.02/.04/.05	RRIYDLIEL	3	1
EBNA-3C	249-258	B27.05	LRGKWQRRYR	3	1
EBNA-3C	271-278	B39	HHIWQNLL	3	1
EBNA-1	407-417	B35.01	HPVGEADYFEY	3	1
EBNA-3C	163-171	B44.03	EGGVGWRHW	3	1
EBNA-3C	343-351	B27.05	FRKAQIQGL	4	1
EBNA-3C	281-290	B44.02	EENLLDFVRF	4	1
EBNA-3C	335-343	B44.02	KEHVIQNAF	4	1
EBNA-3C	213-222	B62	QNGALAINTF	4	1
LMP-2	426-434	A2.01	CLGGLLTMV	4	1
LMP-2	453-461	A2.06	LTAGFLIFL	4	1
LMP-2	131-139	A23	PYLFWLAAI	4	1
LMP-2	442-451	A25	VMSNTLLSAW	4	1
LMP-2	236-244	B27.04	RRRWRRLTV	4	1
LMP-2	200-208	B40	IEDPPFNSL	4	1
BMLF-1	280-288	A2.01	GLCTLVAML	5	2
BZLF-1	54-64	B35	EPLPQGQLTAY	5	2
BZLF-1	190-197	B8	RAKFKQLL	5	2

Supplemental Table 2. Sequences of MHC-class II-restricted EBV epitopes used in intracellular cytokine staining (ICS) and ELISpot IFNγ assays.

33 11-20 mer MHC-class II-restricted epitopes were divided in 3 peptide pools

Protein	Epitope	Sequence	Pools for ELISpot IFNγ	ICS #Tube
EBNA-1	515-528	TSLYNLRRGTALAI	1	3
EBNA-1	499-513	DGGRRKKGGWFGRHR	1	3
EBNA-1	485-499	LRALLARSHVERTTD	1	3
EBNA-1	475-489	NPKFENIAEGLRALL	1	3
EBNA-1	529-543	PQCRLTPLSRLPFGM	1	3
EBNA-1	405-419	RPFFHPVGEADYFEY	1	3
EBNA-1	71-85	RRPQKRPSCIGCKGT	1	3
BHRF-1	171-189	AGLTLSLLVICSYLFISRG	1	3
EBNA-1	55-74	KTSLYNLRRGIALAIPQCRL	1	3
EBNA-1	589-608	PTCNIKATVCSFDDGVDLPP	1	3
EBNA-1	429-448	VPPGAIEQGPADDPGEGPST	1	3
EBNA-2	317-327	TVFYNIPPMPL	2	3
EBNA-1	607-621	MVFLQTHIFAEVLKD	2	3
EBNA-1	519-533	NLRRGTALAIPQCRL	2	3
EBNA-3C	1007-1021	PSMPFASDYSQGAFT	2	3
EBNA-3C	386-400	SDDELPYIDPNMEPV	2	3
EBNA-1	509-528	VYGGSKTSLYNLRRGTALAI	2	3
EBNA-1	588-607	APGPGPQPGPLRESIVCYFM	2	3
EBNA-1	598-617	LRESIVCYFMVFLQTHIFAE	2	3
EBNA-1	618-637	VLKDAIKDLVMTKPAPTCNI	2	3
EBNA-1	594-613	RVTVCSFDDGVDLPPWFPPM	2	3
EBNA-1	426-445	DGEPDMPPGAIEQGPADDPG	2	3
LMP-2	385-398	STEFIPNLFCMLLL	3	3
EBNA-3C	141-155	ILCFVMAARQRLQDI	3	3
LMP-1	130-144	LWRLGATIWQLLAFF	3	3
EBNA-3C	586-600	PPAAGPPAAGPRILA	3	3
EBNA-3C	626-640	PPVVRMFMRERQLPQ	3	3
EBNA-3C	646-660	PQCFWEMRAGREITQ	3	3
EBNA-3C	546-560	QKRAAPPTVSPSDTG	3	3
EBNA-3C	401-415	QQRPVMFVSRVPAKK	3	3
LMP-1	16-30	SGHESDSNSNEGRHH	3	3
LMP-1	15-29	TDGGGGHSHDSGHGG	3	3
EBNA-3C	1052-1067	AQEILSDNSEISVFPK	3	3

Supplemental Table 3. Sequences of BZLF-1 overlapping peptides used in intracellular cytokine staining (ICS) and ELISpot IFNγ assays.

47 15mer peptides overlapping by 10 amino acids and covering the BZLF-1 protein were divided in 5 peptide pools

Protein	Location (HLA class I)	Sequence	Pools for ELISpot IFNγ	ICS Tube #
BZLF-1	1-15	MMDPNSTSEDVKFTP	1	2
BZLF-1	6-20	STSEDVKFTPDPYQV	1	2
BZLF-1	11-25	VKFTPDPYQVPFVQA	1	2
BZLF-1	16-30	DPYQVPFVQAFDQAT	1	2
BZLF-1	21-35	PFVQAFDQATRVYQD	1	2
BZLF-1	26-40	FDQATRVYQDLGGPS	1	2
BZLF-1	31-45	RVYQDLGGPSQAPLP	1	2
BZLF-1	36-50	LGGPSQAPLPCVLWP	1	2
BZLF-1	41-55	QAPLPCVLWPVLPEP	1	2
BZLF-1	46-60	CVLWPVLPEPLPQGQ	1	2
BZLF-1	51-65	VLPEPQGQLTAYH	2	2
BZLF-1	56-70	LPQGQLTAYHVSTAP	2	2
BZLF-1	61-75	LTAYHVSTAPTGSWF	2	2
BZLF-1	66-80	VSTAPTGWFSAPQP	2	2
BZLF-1	71-85	TGSWFSAPQPAPENA	2	2
BZLF-1	76-90	SAPQPAPENAYQAYA	2	2
BZLF-1	81-95	APENAYQAYAAPQLF	2	2
BZLF-1	86-100	YQAYAAPQLFPVSDI	2	2
BZLF-1	91-105	APQLFPVSDITQNQQ	2	2
BZLF-1	96-110	PVSDITQNQQTNQAG	2	2
BZLF-1	101-115	TQNQQTNQAGGEAPQ	3	2
BZLF-1	106-120	TNQAGGEAPQPGDNS	3	2
BZLF-1	111-125	GEAPQPGDNSTVQTA	3	2
BZLF-1	116-130	PGDNSTVQTAAAVVF	3	2
BZLF-1	121-135	TVQTAAAVVFACPGA	3	2
BZLF-1	126-140	AAVVFACPGANQGQQ	3	2
BZLF-1	131-145	ACPGANQGQQLADIG	3	2
BZLF-1	136-150	NQGQQLADIGVPQPA	3	2
BZLF-1	141-155	LADIGVPQPAPVAAP	3	2
BZLF-1	146-160	VPQAPVAAPARRTR	3	2
BZLF-1	151-165	PVAAPARRTRKPQQP	4	2
BZLF-1	156-170	ARRTRKPQQPESLEE	4	2
BZLF-1	161-175	KPQQPESLEECDSEL	4	2
BZLF-1	166-180	ESLEECDSELEIKRY	4	2
BZLF-1	171-185	CDSELEIKRYKNRVA	4	2
BZLF-1	176-190	EIKRYKNRVASRKCR	4	2
BZLF-1	181-195	KNRVASRKCRAKFKQ	4	2
BZLF-1	186-200	SRKCRAKFKQLLQHY	4	2
BZLF-1	191-205	AKFKQLLQHYREVAA	4	2
BZLF-1	196-210	LLQHYREVAAAKSSE	4	2
BZLF-1	201-215	REVAAAKSSENDRLR	5	2
BZLF-1	206-220	AKSSENDRLRLLLKQ	5	2
BZLF-1	211-225	NDRLRLLLKQMCPSL	5	2
BZLF-1	216-230	LLLKQMCPSLDVDSI	5	2
BZLF-1	221-235	MCPSLDVDSIIPRTP	5	2
BZLF-1	226-240	DVDSIIPRTPDVLHE	5	2
BZLF-1	230-245	IPRTPDVLHEDLLNF	5	2

Supplemental Table 4. Sequences of EBNA-3A overlapping peptides used in ELISpot IFNγ assay.

160 15mer peptides overlapping by 10 amino acids and partially covering the EBNA-3A protein were divided in 16 pools

Protein	Location	Sequence	Pool	Protein	Location	Sequence	Pool
EBNA-3A	133 - 147	MYIMYAMAIRQAIRD	1	EBNA-3A	533 - 547	MPVEP VPVPT VALER	9
EBNA-3A	138 - 152	AMAIRQAIRDRRRNP	1	EBNA-3A	538 - 552	VPVPT VALER PVYPK	9
EBNA-3A	143 - 157	QAIRDRRRNPASRRD	1	EBNA-3A	543 - 557	VALER PVYPK PVRPA	9
EBNA-3A	148 - 162	RRRNP ASRRD QAKWR	1	EBNA-3A	548 - 562	PVYPK PVRPA PPLIA	9
EBNA-3A	153 - 167	ASRRD QAKWR LQTLA	1	EBNA-3A	553 - 567	PVRPA PPLIA MQGPG	9
EBNA-3A	158 - 172	QAKWR LQTLA AGWPM	1	EBNA-3A	558 - 572	PPLIA MQGPG ETSGI	9
EBNA-3A	163 - 177	LQTLA AGWPM GYQAY	1	EBNA-3A	563 - 577	MQGPG ETSGI RRARE	9
EBNA-3A	168 - 182	AGWPM GYQAY SSWMY	1	EBNA-3A	568 - 582	ETSGI RRARE RWRPA	9
EBNA-3A	173 - 187	GYQAY SSWMY SYTDH	1	EBNA-3A	573 - 587	RRARE RWRPA PWTPN	9
EBNA-3A	178 - 192	SSWMY SYTDH QTTPT	1	EBNA-3A	578 - 592	RWRPA PWTPN PPRSP	9
EBNA-3A	183 - 197	SYTDH QTTPT FVHLQ	2	EBNA-3A	583 - 597	PWTPN PPRSP SQMSV	10
EBNA-3A	188 - 202	QTTPT FVHLQ ATLGC	2	EBNA-3A	588 - 602	PPRSP SQMSV RDRLA	10
EBNA-3A	193 - 207	FVHLQ ATLGC TGGRR	2	EBNA-3A	593 - 607	SQMSV RDRLA RLRAE	10
EBNA-3A	198 - 212	ATLGC TGGRR CHVTF	2	EBNA-3A	598 - 612	RDRLA RLRAE AQVKQ	10
EBNA-3A	203 - 217	TGGRR CHVTF SAGTF	2	EBNA-3A	603 - 617	RLRAE AQVKQ ASVEV	10
EBNA-3A	208 - 222	CHVTF SAGTF KLPRC	2	EBNA-3A	608 - 622	AQVKQ ASVEV QPPQL	10
EBNA-3A	213 - 227	SAGTF KLPRC TPGDR	2	EBNA-3A	613 - 627	ASVEV QPPQL TQVSP	10
EBNA-3A	218 - 232	KLPRC TPGDR QWLYV	2	EBNA-3A	618 - 632	QPPQL TQVSP QQPME	10
EBNA-3A	223 - 237	TPGDR QWLYV QSSVG	2	EBNA-3A	623 - 637	TQVSP QQPME GPLVP	10
EBNA-3A	228 - 242	QWLYV QSSVG NIVQS	2	EBNA-3A	628 - 642	QQPME GPLVP EQQMF	10
EBNA-3A	233 - 247	QSSVG NIVQS CNPRY	3	EBNA-3A	633 - 647	GPLVP EQQMF PGAPF	11
EBNA-3A	238 - 252	NIVQS CNPRY SIFFD	3	EBNA-3A	638 - 652	EQQMF PGAPF SQVAD	11
EBNA-3A	243 - 257	CNPRY SIFFD YMAIH	3	EBNA-3A	643 - 657	PGAPF SQVAD VVRAP	11
EBNA-3A	248 - 262	SIFFD YMAIH RSLTK	3	EBNA-3A	648 - 662	SQVAD VVRAP GVPAM	11
EBNA-3A	253 - 267	YMAIH RSLTK IWEEV	3	EBNA-3A	653 - 667	VVRAP GVPAM QPQYF	11
EBNA-3A	258 - 272	RSLTK IWEEV LTPDQ	3	EBNA-3A	658 - 672	GVPAM QPQYF DLPLI	11
EBNA-3A	263 - 277	IWEEV LTPDQ RVSFM	3	EBNA-3A	663 - 677	QPQYF DLPLI QPISQ	11
EBNA-3A	268 - 282	LTPDQ RVSFM EFLGF	3	EBNA-3A	668 - 682	DLPLI QPISQ GAPVA	11
EBNA-3A	273 - 287	RVSFM EFLGF LQRTD	3	EBNA-3A	673 - 687	QPISQ GAPVA PLRAS	11
EBNA-3A	278 - 292	EFLGF LQRTD LSYIK	3	EBNA-3A	678 - 692	GAPVA PLRAS MGPVP	11
EBNA-3A	283 - 297	LQRTD LSYIK SFVSD	4	EBNA-3A	683 - 697	PLRAS MGPVP PVPAT	12
EBNA-3A	288 - 302	LSYIK SFVSD ALGTT	4	EBNA-3A	688 - 702	MGPVP PVPAT QPQYF	12
EBNA-3A	293 - 307	SFVSD ALGTT SIQTP	4	EBNA-3A	693 - 707	PVPAT QPQYF DIPLT	12
EBNA-3A	298 - 312	ALGTT SIQTP WIDDN	4	EBNA-3A	698 - 712	QPQYF DIPLT EPINQ	12
EBNA-3A	303 - 317	SIQTP WIDDN PSTET	4	EBNA-3A	703 - 717	DIPLT EPINQ GASAA	12
EBNA-3A	308 - 322	WIDDN PSTET AQAWN	4	EBNA-3A	708 - 722	EPINQ GASAA HFLPQ	12
EBNA-3A	313 - 327	PSTET AQAWN AGFLR	4	EBNA-3A	713 - 727	GASAA HFLPQ QPMEG	12
EBNA-3A	318 - 332	AQAWN AGFLR GRAYG	4	EBNA-3A	718 - 732	HFLPQ QPMEG PLVPE	12
EBNA-3A	323 - 337	AGFLR GRAYG IDLLR	4	EBNA-3A	723 - 737	QPMEG PLVPE QWMFP	12
EBNA-3A	328 - 342	GRAYG IDLLR TEGEH	4	EBNA-3A	728 - 742	PLVPE QWMFP GAALS	12
EBNA-3A	333 - 347	IDLLR TEGEH VEGAT	5	EBNA-3A	733 - 747	QWMFP GAALS QSVRP	13
EBNA-3A	338 - 352	TEGEH VEGAT GETRE	5	EBNA-3A	738 - 752	GAALS QSVRP GVAQS	13
EBNA-3A	343 - 357	VEGAT GETRE ESEDT	5	EBNA-3A	743 - 757	QSVRP GVAQS QYFDL	13
EBNA-3A	348 - 362	GETRE ESEDT ESDGD	5	EBNA-3A	748 - 762	GVAQS QYFDL PLTQP	13
EBNA-3A	353 - 367	ESEDT ESDGD DEDELP	5	EBNA-3A	753 - 767	QYFDL PLTQP INHGA	13
EBNA-3A	358 - 372	ESDGD DEDELP CIVSR	5	EBNA-3A	758 - 772	PLTQP INHGA PAAHF	13
EBNA-3A	363 - 377	DEDELP CIVSR GGPKV	5	EBNA-3A	763 - 777	INHGA PAAHF LHQPP	13
EBNA-3A	368 - 382	CIVSR GGPKV KRPPI	5	EBNA-3A	768 - 782	PAAHF LHQPP MEGPW	13
EBNA-3A	373 - 387	GGPKV KRPPI FIRRL	5	EBNA-3A	773 - 787	LHQPP MEGPW VPEQW	13
EBNA-3A	378 - 392	KRPPI FIRRL HRLLL	5	EBNA-3A	778 - 792	MEGPW VPEQW MFQGA	13
EBNA-3A	383 - 397	FIRRL HRLLL MRAGK	6	EBNA-3A	783 - 797	VPEQW MFQGA PPSQG	14
EBNA-3A	388 - 402	HRLLL MRAGK RTEQG	6	EBNA-3A	788 - 802	MFQGA PPSQG TDVVQ	14
EBNA-3A	393 - 407	MRAGK RTEQG KEVLE	6	EBNA-3A	793 - 807	PPSQG TDVVQ HQLDA	14
EBNA-3A	398 - 412	RTEQG KEVLE KARGS	6	EBNA-3A	798 - 812	TDVVQ HQLDA LGYTL	14

EBNA-3A	403	-	417	KEVLE KARGS TYGTP	6	EBNA-3A	803	-	817	HQLDA LGYTL HGLNH	14
EBNA-3A	408	-	422	KARGS TYGTP RPPVP	6	EBNA-3A	808	-	822	LGYTL HGLNH PGVPV	14
EBNA-3A	413	-	427	TYGTP RPPVP KPRPE	6	EBNA-3A	813	-	827	HGLNH PGVPV SPAVN	14
EBNA-3A	418	-	432	RPPVPKPRPEVPQSD	6	EBNA-3A	818	-	832	PGVPV SPAVN QYHLS	14
EBNA-3A	423	-	437	KPRPE VPQSD ETATS	6	EBNA-3A	823	-	837	SPAVN QYHLS QAAFG	14
EBNA-3A	428	-	442	VPQSD ETATS HGSAQ	6	EBNA-3A	828	-	842	QYHLS QAAFG LPIDE	14
EBNA-3A	433	-	447	ETATS HGSAQ VPEPP	7	EBNA-3A	833	-	847	QAAFG LPIDE DESGE	15
EBNA-3A	438	-	452	HGSAQ VPEPP TIHLA	7	EBNA-3A	838	-	852	LPIDE DESGE GSDTS	15
EBNA-3A	443	-	457	VPEPP TIHLA AQGMA	7	EBNA-3A	843	-	857	DESGE GSDTS EPCEA	15
EBNA-3A	448	-	462	TIHLA AQGMA YPLHE	7	EBNA-3A	848	-	862	GSDTS EPCEA LDLSI	15
EBNA-3A	453	-	467	AQGMA YPLHE QHGMA	7	EBNA-3A	853	-	867	EPCEA LDLSI HGRPC	15
EBNA-3A	458	-	472	YPLHE QHGMA PCPVA	7	EBNA-3A	858	-	872	LDLSI HGRPC PQAPE	15
EBNA-3A	463	-	477	QHGMA PCPVA QAPPT	7	EBNA-3A	863	-	877	HGRPC PQAPE WPVQE	15
EBNA-3A	468	-	482	PCPVA QAPPT PLPPV	7	EBNA-3A	868	-	882	PQAPE WPVQE EGGQD	15
EBNA-3A	473	-	487	QAPPT PLPPV SPGDQ	7	EBNA-3A	873	-	887	WPVQE EGGQD ATEVL	15
EBNA-3A	478	-	492	PLPPV SPGDQ LPGVF	7	EBNA-3A	878	-	892	EGGQD ATEVL DLSIH	15
EBNA-3A	483	-	497	SPGDQ LPGVF SDGRV	8	EBNA-3A	883	-	897	ATEVL DLSIH GRPRP	16
EBNA-3A	488	-	502	LPGVF SDGRV ACAPV	8	EBNA-3A	888	-	902	DLSIH GRPRP RTPEW	16
EBNA-3A	493	-	507	SDGRV ACAPV PAPAG	8	EBNA-3A	893	-	907	GRPRP RTPEW PVQGE	16
EBNA-3A	498	-	512	ACAPV PAPAG PIVRP	8	EBNA-3A	898	-	912	RTPEW PVQGE GGQNV	16
EBNA-3A	503	-	517	PAPAG PIVRP WEPSL	8	EBNA-3A	903	-	917	PVQGE GGQNV TGPET	16
EBNA-3A	508	-	522	PIVRP WEPSL TQAAG	8	EBNA-3A	908	-	922	GGQNV TGPET RRVVV	16
EBNA-3A	513	-	527	WEPSL TQAAG QAFAP	8	EBNA-3A	913	-	927	TGPET RRVVV SAVVH	16
EBNA-3A	518	-	532	TQAAG QAFAP VRPQH	8	EBNA-3A	918	-	932	RRVVV SAVVH MCQDD	16
EBNA-3A	523	-	537	QAFAP VRPQH MPVEP	8	EBNA-3A	923	-	937	SAVVH MCQDD EFPDL	16
EBNA-3A	528	-	542	VRPQH MPVEP VPVPT	8	EBNA-3A	928	-	944	MCQDD EFPDL QDPPDEA	16

Supplemental Table 5. Univariate analysis of prognostic factors for PTLD outcome

Overall survival				
	EBV-neg PTLD		**EBV-pos PTLD**	
Variable	**HR (95% CI)**	**P**	**HR (95% CI)**	**P**
Age ≥60 years*	0.28 (0.089-0.9)	**0.032**	0.51 (0.19-1.3)	0.173
PTLD localization (CNS vs systemic)	nd†		0.49 (0.18-1.3)	0.166
Elevated LDH*	1.4 (0.52-4)	0.485	0.21 (0.05-0.94)	**0.041**
Monomorphic PTLD (vs polymorphic)	nd‡		0.5 (0.11-2.2)	0.361
Early-onset (≤1 year vs >1 year)	0.18 (0.02-1.5)	0.117	1.2 (0.35-4.3)	0.755
CD4 lymphopenia * (≤300 cells/mm^3)	0.1 (0.02-0.44)	**0.002**	0.53 (0.19-1.5)	0.233
≥5%TIM-3$^+$ CD4$^+$ T cells (vs <5%)*	0.43 (0.13-1.3)	0.146	0.55 (0.19-1.6)	0.274
Transplant type (kidney vs others)				
Liver	0.66(0.17-2.55)	0.546	0.99 (0.28-3.50)	0.982
Thoracic	1.99(0.50-7.83)	0.326	0.51 (0.11-2.28)	0.376
Multiple	3.37(0.68-16.68)	0.137		
Progression-free survival				
	EBV-neg PTLD		**EBV-pos PTLD**	
Variable	**HR (95% CI)**	**P**	**HR (95% CI)**	**P**
Age ≥60 years*	0.39 (0.13-1.1)	0.082	0.48 (0.19-1.3)	0.13
PTLD localization (CNS vs systemic)	nd†		0.56 (0.22-1.5)	0.24
Elevated LDH*	1.2 (0.46-3.3)	0.69	0.31 (0.089-1.1)	0.071
Monomorphic PTLD (vs polymorphic)	nd‡		0.48 (0.11-2.1)	0.32
Early-onset (≤1 year vs >1 year)	0.26 (0.032-2.1)	0.2	0.94 (0.31-2.8)	0.91
CD4 lymphopenia * (≤300 cells/mm^3)	0.07 (0.02-0.35)	**<0.001**	0.63 (0.23-1.7)	0.35
≥5%TIM-3$^+$ CD4$^+$ T cells (vs <5%)*	0.36 (0.12-1.1)	0.076	0.54 (0.18-1.6)	0.26
Transplant type (kidney vs others)				
Liver	1.01 (0.29-3.50)	0.978	1.28(0.41-3.9)	0.665
Thoracic	1.95 (0.49-7.64)	0.338	0.49(0.11-2.22)	0.359
Multiple	3.37 (0.68-16.61)	0.135		

*at PTLD diagnosis; HR, Hazard ratio; nd, not determined ; †all EBV-neg PTLDs were monomorphic ; ‡only one EBV-neg PTLD had central nervous system (CNS) disease.

Supplemental Table 6. Multivariable Cox-regression analysis of overall survival in EBV-neg PTLDs

Cox-regression model n=38 , Likelihood ratio test P<0.0001

Variable	HR (95% CI)	P
Age ≥60 years*	0.27 (0.08-0.86)	**0.027**
CD4 lymphopenia * (≤300 cells/mm^3)	0.09 (0.02-0.44)	**0.002**

Supplemental Table 7. Predicted and detected T cell responses of transplant controls (TC), EBV-positive (EBV+PTLD) and EBV-negative (EBV-PTLD) PTLD patients against class-II MHC, BZLF-1 and EBNA-3A peptide pools

Patient ID	class II-HLA alleles	EBV peptide pools																								
		class II-MHC restricted			BZLF-1					EBNA-3A																
		1	2	3	1	2	3	4	5	1	2	3	4	5	6	7	8	9	10	11	12	13	14	15	16
TC 8	DR ?-7	●	●	●	n	n	n	n	n	n	n	n	n	n	n	n	n	n	n	n	n	n	n	n	n
TC 9	NA	●	●		n	n	n	n	n	n	n	n	n	n	n	n	n	n	n	n	n	n	n	n	n
TC 11	NA			●	n	n	n	n	n	n	n	n	n	n	n	n	n	n	n	n	n	n	n	n	n
TC 14	NA			●			●			n	n	n	n	n	n	n	n	n	n	n	n	n	n	n	n
TC 2	NA								●									●							
TC 3	DR 10-15							●		●			●	●	●										
TC 4	DR 07-13		●		●	●	●	●				●	●	●	●										
TC 5	DR 17-7 DQ 2-0													●											
TC 7	DR 17-13 DQ 2-6				●																				
TC 10	DR 1-0 DQ 5-?					●										●									
TC18	NA							●			●														
TC 1	DR 15-4	n	n	n				●																	
TC 21	NA	n	n	n																					
TC 24	NA	n	n	n				●			●														
TC 26	NA	n	n	n				●		●															
TC 27	NA	n	n	n			●				●									●					
EBV+PTLD 2	NA	●	●	●	n	n	n	n	n	n	n	n	n	n	n	n	n	n	n	n	n	n	n	n	n
EBV+PTLD 18	DR 1-11				n	n	n	n	n	n	n	n	n	n	n	n	n	n	n	n	n	n	n	n	n
EBV+PTLD 19	DR 3-4 DQ 2-3				n	n	n	n	n	n	n	n	n	n	n	n	n	n	n	n	n	n	n	n	n
EBV+PTLD 4	DR 13-9 DQ 1-3	●	●	●				●	●	n	n	n	n	n	n	n	n	n	n	n	n	n	n	n	n
EBV+PTLD 20	NA			●				●																	
EBV+PTLD 3	DR 15-4	n	n	n																					
EBV+PTLD 5	DR 9-11 DQ 2-3	n	n	n				●																	
EBV+PTLD 16	DR 12-13 DQ 3-6	n	n	n				●																	
EBV+PTLD 30	DR 17-15	n	n	n				●																	
EBV+PTLD 36	DR 17-15 DQ 17-15	n	n	n				●																	
EBV+PTLD 37	DR 17-13 DQ 2-6	n	n	n			●		●																

EBV+PTLD 43	DR 7-11 DQ 2-7	n	n	n	●		●												●						●
EBV+PTLD 9	NA	n	n	n			●			●				●				●							●
EBV+PTLD 22	NA	n	n	n																					
EBV+PTLD 24	NA	n	n	n																					
EBV+PTLD 26	NA	n	n	n			●																		
EBV+PTLD 27	NA	n	n	n			●																		
EBV+PTLD 29	NA	n	n	n				●																	
EBV+PTLD 38	NA	n	n	n				●									●			●					
EBV+PTLD 42	NA	n	n	n																					
EBV+PTLD 44	NA	n	n	n				●																	
EBV+PTLD 47	NA	n	n	n																					●
EBV-PTLD 0	DR 13-14 DQ 5-6				●			●			●														
EBV-PTLD 1	DR 14-15 DQ 5-6				●	●	●		●	●	●	●	●		●	●	●	●							●
EBV-PTLD 2	DR 1-3 DQ 2-5	●	●	●		●										●									
EBV-PTLD 3	NA	●														●									
EBV-PTLD 5	DR 4-4 DQ 3-3			●																					
EBV-PTLD 9	DR 3-5	●						●						●		●									
EBV-PTLD 10	DR 4-14			●				●		●		●	●							●					
EBV-PTLD 11	NA																								
EBV-PTLD 13	DR 4-7 DQ 2-8	n	n	n	●			●																	
EBV-PTLD 17	DR 9-11 DQ 9-7	n	n	n										●											
EBV-PTLD 18	NA	n	n	n		●																			
EBV-PTLD 20	NA	n	n	n				●																	
EBV-PTLD 22	NA	n	n	n			●																		
EBV-PTLD 25	NA	n	n	n							●														
EBV-PTLD 26	NA	n	n	n	●						●	●	●	●				●				●			
EBV-PTLD 28	NA	n	n	n	●				●	●															●
EBV-PTLD 30	NA	n	n	n																					
EBV-PTLD 32	NA	n	n	n				●		●							●			●					
EBV-PTLD 33	NA	n	n	n			●																		
EBV-PTLD 39	NA	n	n	n																					

EBV-specific T cell responses were studied by ELISpot IFNγ. Black dots (●) indicate a responses was detected against that peptide pool. Green background (■) indicate pools where at least one known epitope was restricted to patient HLA. BZLF-1 and EBNA-3A 15-mers binding to patients HLA were predicted with NetMHCIIpan 4.0. Strong binders (rank <0.5; ■) are mapped in orange and weak binders (rank >0.5 <2; ■) in yellow. NA, not available; n, not tested.

Supplemental Table 8. Predicted and detected T cell responses of transplant controls (TC), EBV-positive (EBV+PTLD) and EBV-negative (EBV-PTLD) PTLD patients against class-I MHC, BZLF-1 and EBNA-3A peptide pools

Patient ID	class I-HLA alleles	EBV peptide pools																									
		class I-MHC restricted					BZLF-1					EBNA-3A															
		1	2	3	4	5	1	2	3	4	5	1	2	3	4	5	6	7	8	9	10	11	12	13	14	15	16
TC 1	A 3-11 B 40-14	●		●						●																	
TC 2	A 28-32 B 07-40				●						●									●							
TC 3	A 28-? B 57-70									●		●			●	●	●										
TC 4	A 2-11 B 27-44			●	●	●	●	●	●	●				●	●	●	●										
TC 5	A 1-2 B 7-?	●														●											
TC 7	A 2-68 B 70-51						●																				
TC 10	A 1-2 B 35-57	●			●	●												●									
TC18	NA	●				●				●			●														
TC 21	NA				●																						
TC 24	NA		●	●	●					●			●														
TC 26	NA					●				●		●															
TC 27	NA	●	●		●				●				●									●					
EBV+PTLD 3	A 24-10 B 75-53																										
EBV+PTLD 5	A 30-30 B 07-08					●				●																	
EBV+PTLD 6	A 01-02 B 10-37		●		●					●	●									●							
EBV+PTLD 9	NA				●				●			●				●				●							●
EBV+PTLD 11	A 02-31 B 15-40		●		●	●			●																		
EBV+PTLD 16	A 33-? B 58-14									●																	
EBV+PTLD 20	NA	□	●	□		□				●																	
EBV+PTLD 22	A 24-33 B 14-58																										
EBV+PTLD 24	NA																										
EBV+PTLD 26	NA		●						●																		
EBV+PTLD 27	NA				●				●																		
EBV+PTLD 29	NA				●				●																		
EBV+PTLD 30	A 29-30 B 44-27									●																	
EBV+PTLD 36	A 3-23 B 44-50				●					●																	
EBV+PTLD 37	A 3-24 B 62-51								●		●																
EBV+PTLD 38	NA		●							●									●			●					
EBV+PTLD 42	NA																										

EBV+PTLD 43	A 2-2 B 13-51	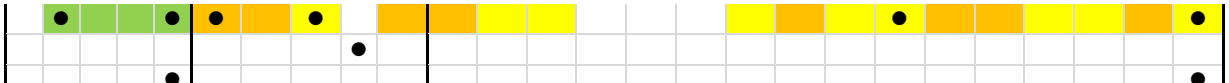
EBV+PTLD 44	NA	
EBV+PTLD 47	NA	
EBV-PTLD 0	A 02-09 B 15-35	
EBV-PTLD 1	A 24-29 B 27-52	
EBV-PTLD 2	A 03-26 B 08-35	
EBV-PTLD 3	NA	
EBV-PTLD 5	A 2-9 B 44-51	
EBV-PTLD 9	A 3-32 B 7-8	
EBV-PTLD 10	A 2-23 B 44-49	
EBV-PTLD 11	A 3-11 B 7-35	
EBV-PTLD 13	A 2-2 B 44-72	
EBV-PTLD 17	A 2-2 B 61-51	
EBV-PTLD 18	NA	
EBV-PTLD 20	NA	
EBV-PTLD 22	NA	
EBV-PTLD 25	NA	
EBV-PTLD 26	NA	
EBV-PTLD 28	NA	
EBV-PTLD 30	NA	
EBV-PTLD 32	NA	
EBV-PTLD 33	NA	
EBV-PTLD 39	NA	

EBV-specific T cell responses were studied by ELISpot IFNγ. Black dots (●) indicate a responses was detected against that peptide pool. Green background (■) indicate pools where at least one known epitope was restricted to patient HLA. BZLF-1 and EBNA-3A 9-mers binding to patients HLA were predicted with NetMHCpan 4.0. Strong binders (rank <0.5; ■) are mapped in orange and weak binders (rank >0.5 <2; ■) in yellow. NA, not available; n, not tested.

Supplemental Figure 1. Flow chart of the study controls

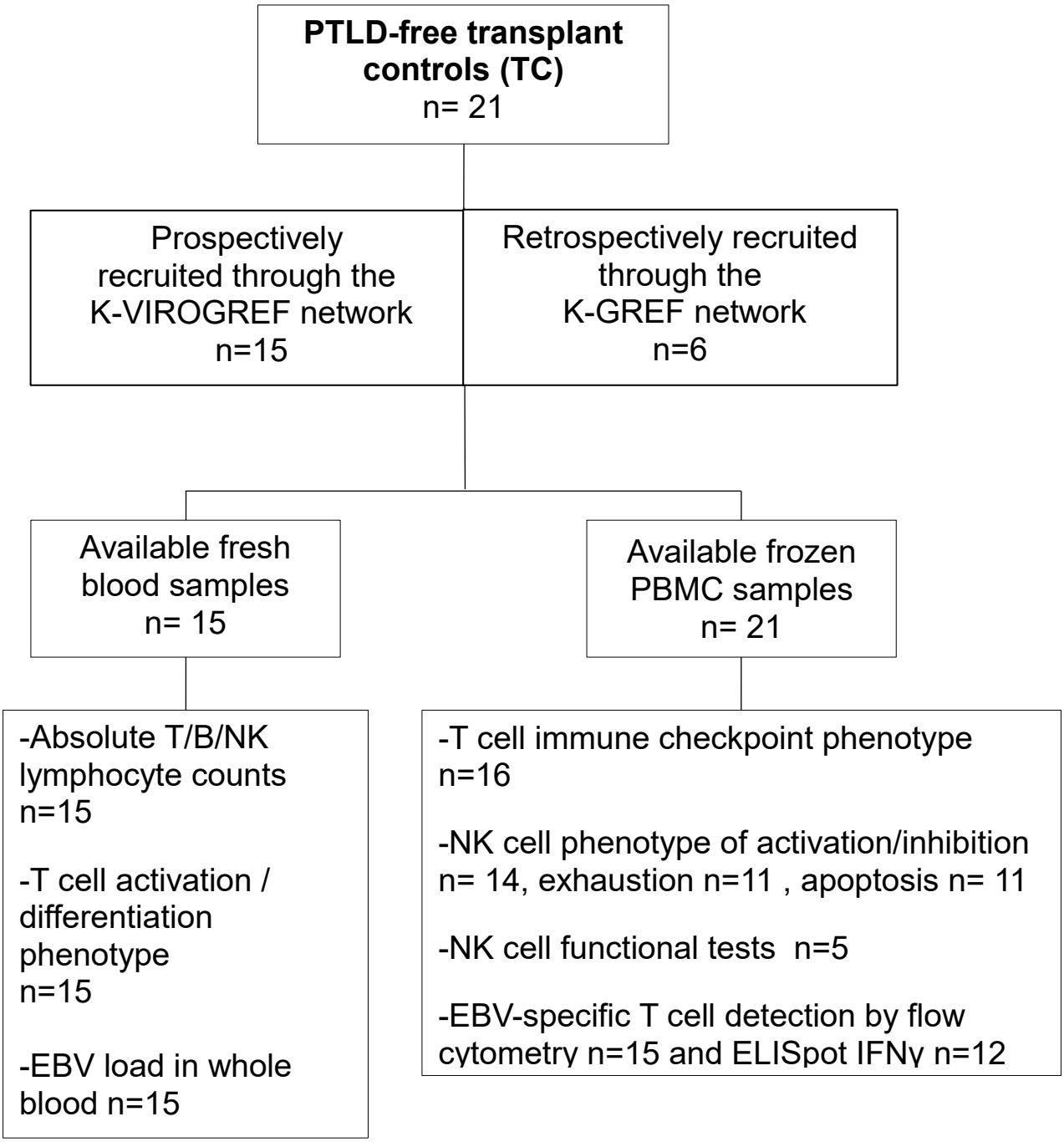

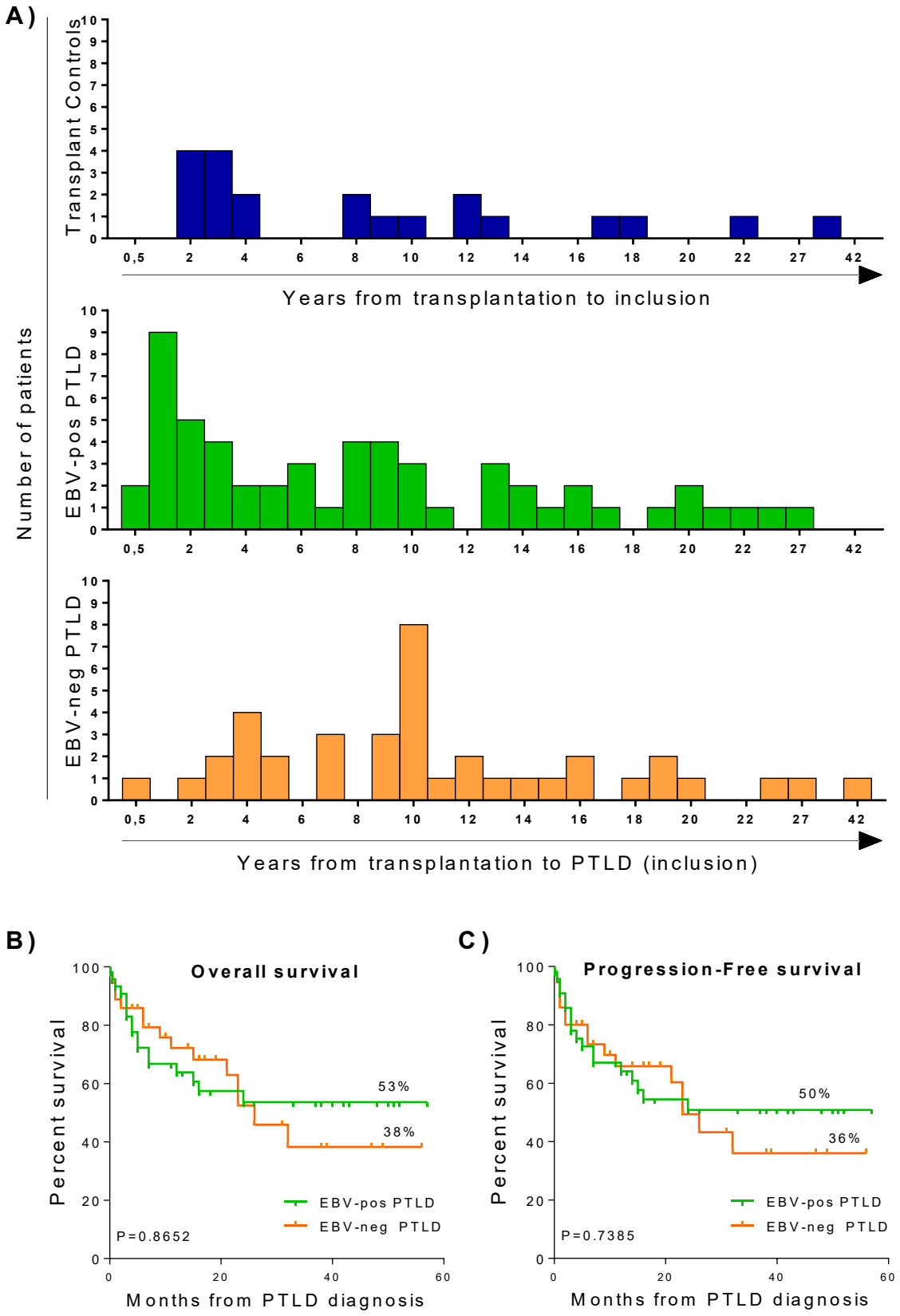

Supplemental Figure 2. Time from transplantation to inclusion and survival of EBV-positive and EBV-negative PTLD patients. (A) Bars represent the number of patients included in relation to the number of years since last transplantation. Data are

shown for 21 PTLD-free controls (upper panel), 56 EBV-positive (middle panel) and 39 EBV-negative (lower panel) PTLD patients. Kaplan Meyer curves of (B) overall and (C) progression-free survival after EBV-positive (green) and EBV-negative (orange) PTLD diagnosis. Overall survival was defined as the time elapsed between PTLD diagnosis and death and Progression-Free survival was defined as the time elapsed between PTLD diagnosis and progression or relapse or death. Patients who were lost of track were censured. Differences in survival between groups were calculated with the Log-rank test followed by false discovery rate correction for multiple tests (FDR=0.05). Only adjusted p-values are shown.

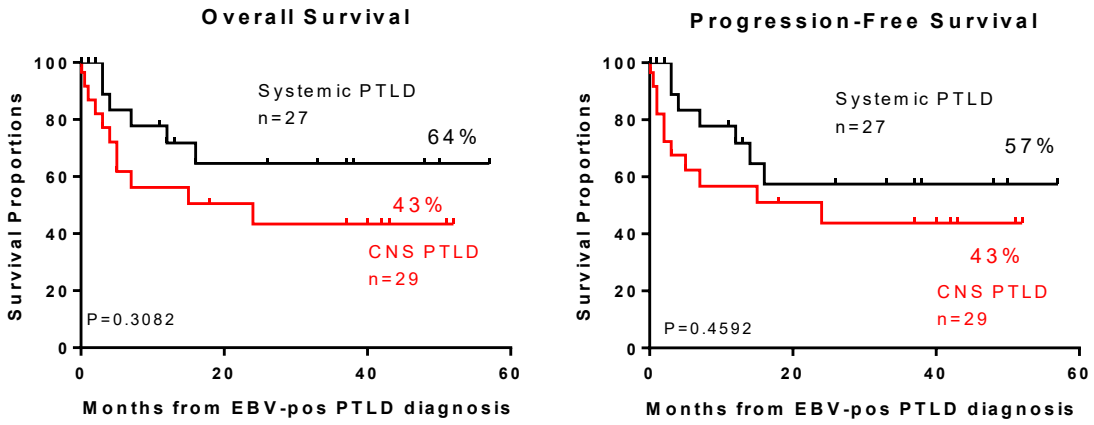

Supplemental Figure 3. EBV-positive PTLD survival in relation to disease location Kaplan Meyer curves of overall survival after (left) and progression-free survival (right) of EBV-positive PTLD patients (EBV-pos) according to disease location. Systemic disease was defined as any nodal or extra-nodal disease regardless of the affected organ outside of central nervous system (CNS). Differences in survival were calculated with the Log-rank test followed by false discovery rate (FDR=0.05) correction for multiple tests. Only adjusted p-values are shown.

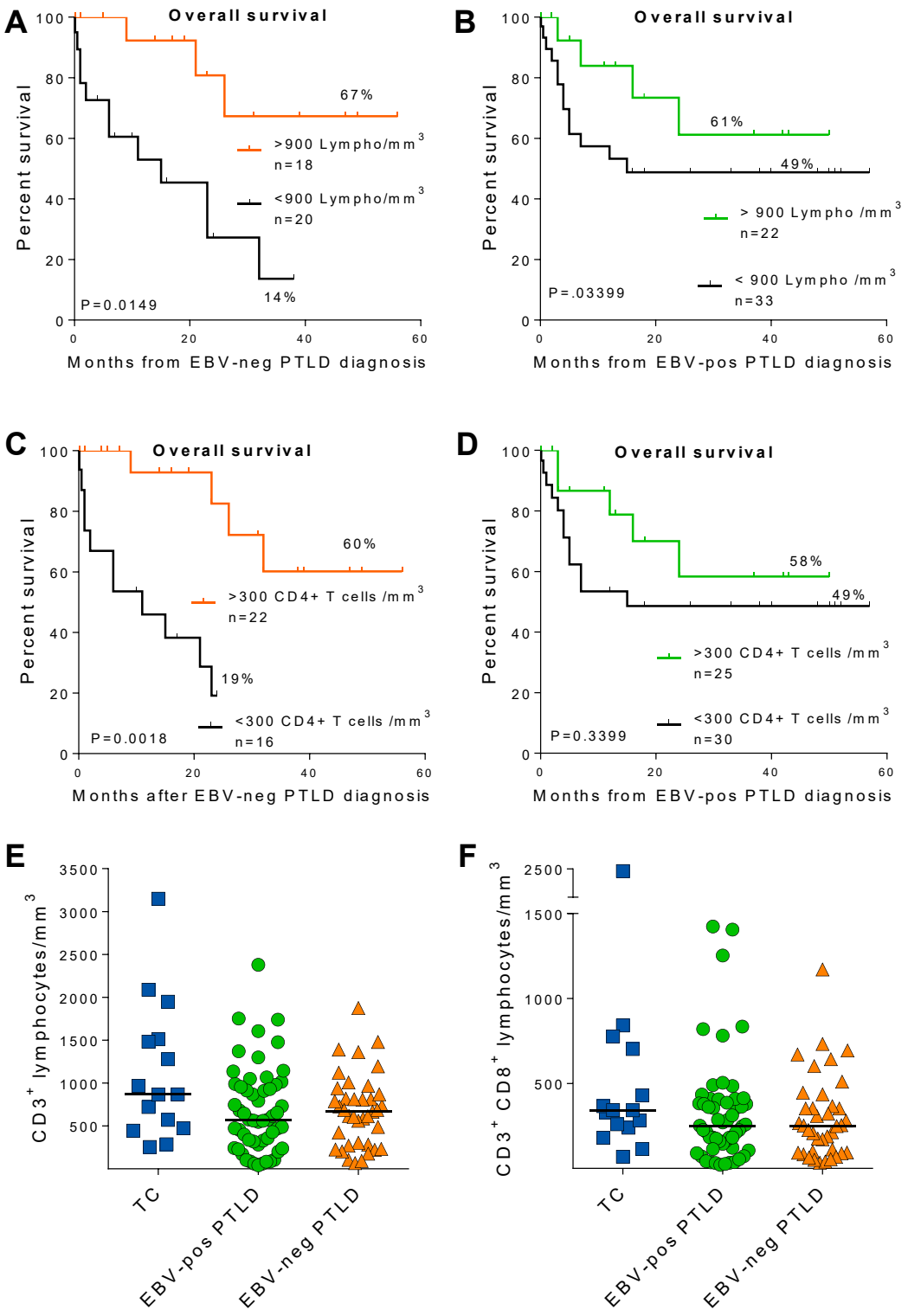

Supplemental Figure 4. Survival in relation to absolute counts of lymphocyte subpopulations in EBV-positive and EBV-negative PTLD patients. (A-D) Kaplan Meyer curves of overall survival after (A and C) EBV-positive or (B and D) EBV-

negative PTLD diagnosis according to upper (colored lines) and lower (black lines) median absolute counts of (A-B) $CD45^+$ lymphocytes or (C-D) $CD4^+$ T cells at PTLD diagnosis. Median count of 108 individual measures among the 3 groups of patients were set as cutoff for Kaplan Meyer curves. Differences in overall survival were calculated with the Log-rank test followed by false discovery rate (FDR=0.05) correction for multiple tests. Individual measures of absolute (E) $CD3^+$ lymphocytes and (F) $CD3^+CD8^+$ lymphocyte counts by group. Horizontal lines in dot plots represent medians, compared between groups with a Kruskall Wallis test and Dunn's multiple comparison post-test. Individual measures are represented as blue squares (■) for TCs, green circles (●) for EBV-positive PTLDs and orange triangles (▲) for EBV-negative PTLDs. Only adjusted p-values are shown.

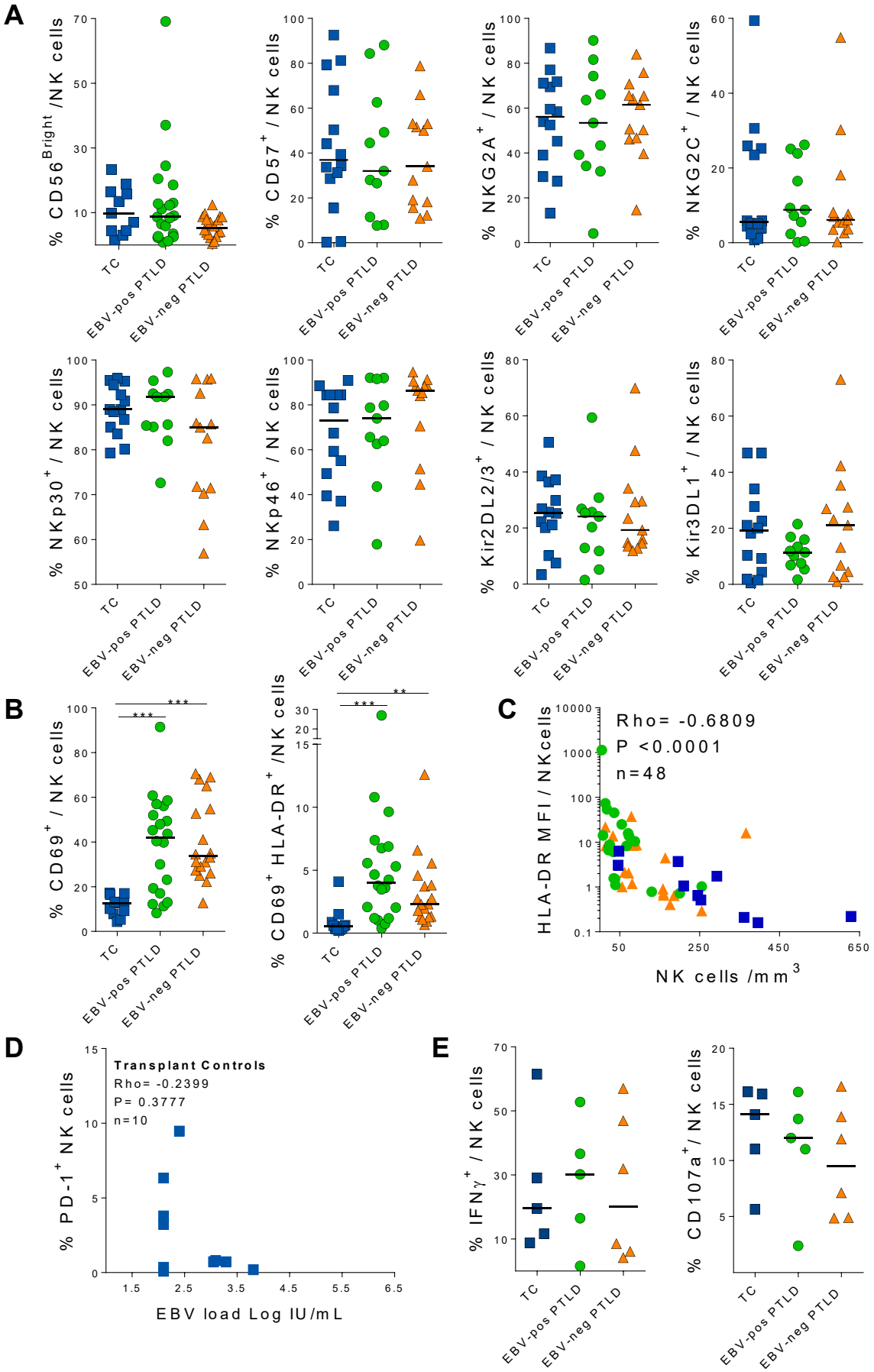
A
% CD56Bright /NK cells
% CD57+ / NK cells
% NKG2A+ / NK cells
% NKG2C+ / NK cells
% NKp30+ / NK cells
% NKp46+ / NK cells
% Kir2DL2/3+ / NK cells
% Kir3DL1+ / NK cells
TC
EBV-pos PTLD
EBV-neg PTLD
B
% CD69+ / NK cells
% CD69+ HLA-DR+ /NK cells
***
**
C
HLA-DR MFI / NKcells
Rho= -0.6809
P <0.0001
n=48
NK cells /mm3
D
% PD-1+ NK cells
Transplant Controls
Rho= -0.2399
P= 0.3777
n=10
EBV load Log IU/mL
E
% IFNγ+ / NK cells
% CD107a+ / NK cells

Supplemental Figure 5.Complementary data of NK cell phenotype from EBV-pos and EBV-neg PTLD patients and transplant controls (TC). (A) Frequencies of $CD56^{Bright}$ NK cells and of $CD3^{-}CD56^{+}$ NK cells expressing CD57 differentiation marker, c-lectin receptors (NKG2A and NKG2C), natural cytotoxicity receptors (NKp30 and NKp46) and killer immunoglobulin receptors (Kir2DL2/3 and Kir3DL1) from14 Transplant controls, 11 EBV-pos and 13 EBV-neg PTLD patients. (B) Frequencies of $CD3^{-}CD56^{+}$ NK cells expressing CD69 or CD69/HLA-DR activation markers were measured in 11 TC, 20 EBV-pos and 18 EBV-neg PTLD patients. (C) Spearman correlation between HLA-DR mean fluorescence intensity (MFI) on total $CD3^{-}$ $CD56^{+}$ NK cells and the number of NK cells/mm3 at inclusion from 10 TC, 19 EBV-pos PTLD and 18 EBV-neg PTLD. (D) Spearman correlation between PD-1 expression (MFI) and EBV load (Log of International Units (IU)/mL) from 10 Transplant controls. (E) Proportion of $IFN\gamma^{+}$ and $CD107a^{+}$ NK cells detected after IL-12/IL-18 stimulation or incubation with K562 targets, respectively, in 5 TC, 5 EBV-pos and 6 EBV-neg PTLD patients. Lines in dot plots represent median values. Groups were compared with two-tailed Mann-Whitney test or Kruskall Wallis test and Dunn's multiple comparison post-test. Individual measures are represented as blue squares (■) for TCs, green circles (●) for EBV-positive PTLDs and orange triangles (▲) for EBV-negative PTLDs.

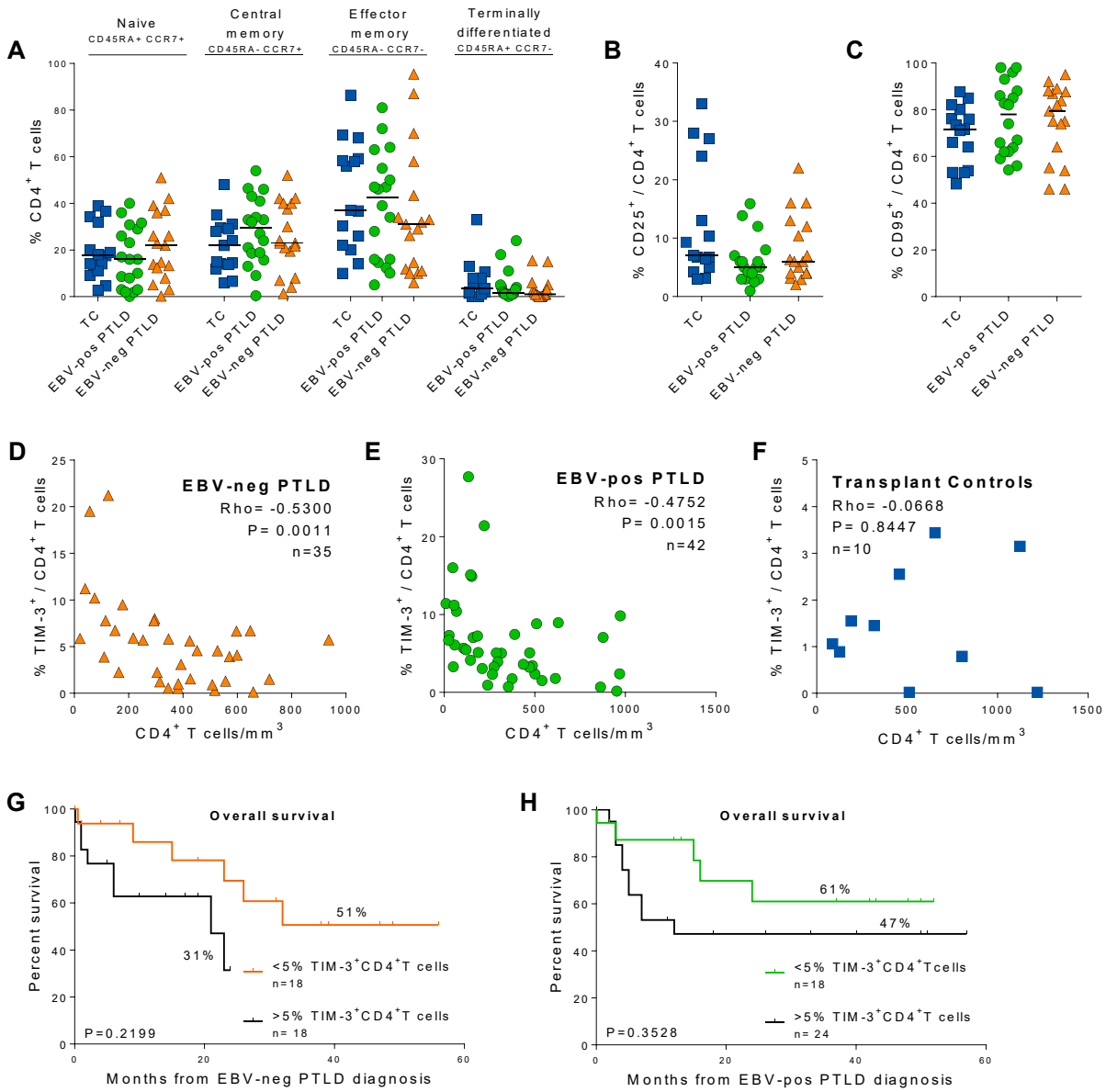

Supplemental Figure 6. Complementary data of CD4⁺ T cell phenotype from EBV-positive and EBV-negative PTLD patients and transplant controls (TC). The CD4⁺ T cell differentiation and activation phenotypes were studied by flow cytometry in whole blood of 15 TC, 18 EBV-pos and 17 EBV-neg PTLD patients. Data are shown for (A) Naïve and memory subsets according to CD45RA and CCR7 expression and (B) CD25 and (C) CD95 surface markers within $CD3^+CD4^+$ lymphocytes. Horizontal lines in dot-plots represent medians. Median values were compared between groups with a Kruskall Wallis test and Dunn's multiple comparison post-test. (D-F) Spearman correlation between the frequency of TIM-3⁺ CD4⁺ T cells and absolute CD4⁺T-cell

counts at inclusion. (G-H) Kaplan Meyer curves of overall survival after (G) EBV-neg and (H) EBV-pos PTLD diagnosis according to upper (colored lines) and lower (black lines) median frequencies of peripheral Tim-3^+ $CD4^+$ T cells. Medians were determined from the 93 individual measures within the 3 groups of patients. Differences in progression-free survival were calculated with the Log-rank test followed by followed by false discovery rate (FDR=0.05) correction for multiple tests. Only adjusted p-values are shown. Individual measures are represented as blue squares (■) for TCs, green circles (●) for EBV-positive PTLDs and orange triangles (▲) for EBV-negative PTLDs..

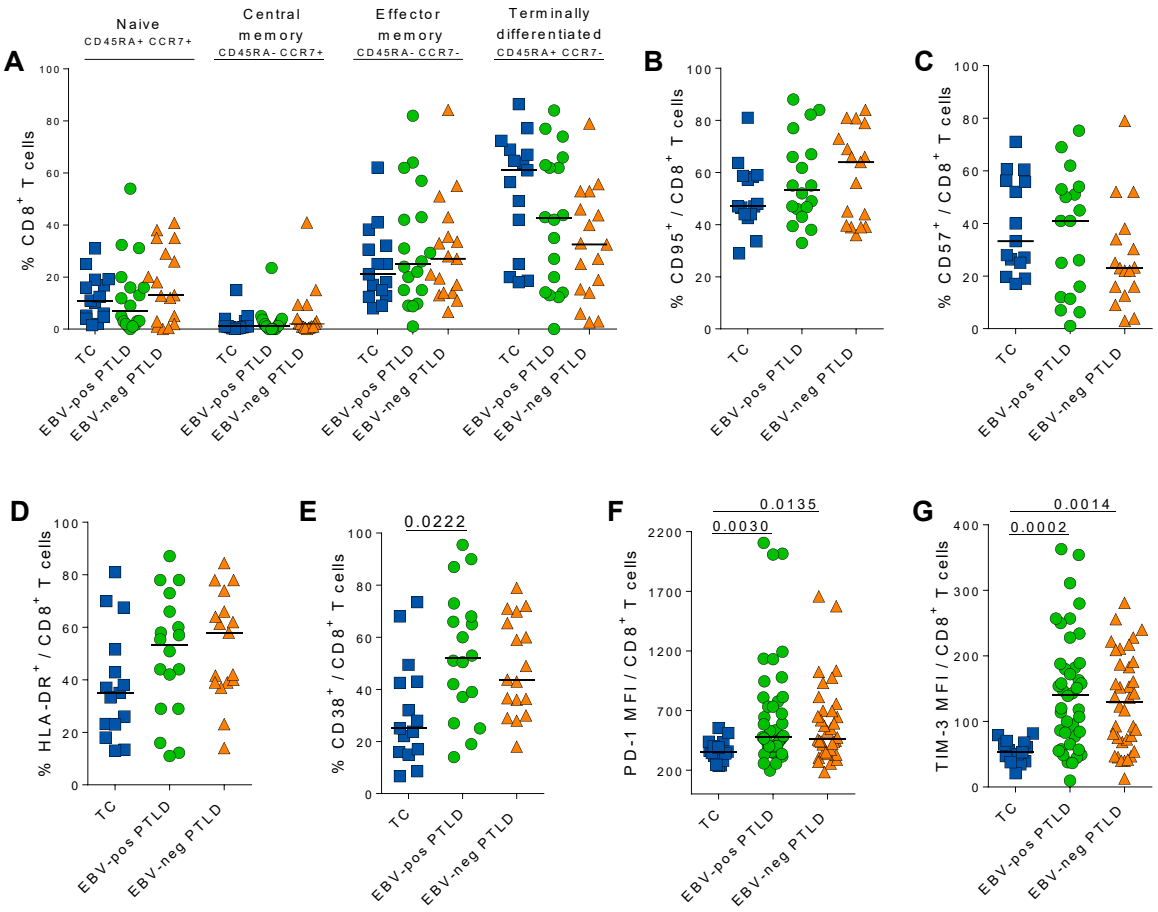

Supplemental Figure 7. Complementary data of CD8⁺ T cell phenotype from EBV-positive and EBV-negative PTLD patients and transplant controls (TC). The CD8⁺ T cell differentiation and activation phenotypes were studied by flow cytometry in whole blood of 15 TC, 18 EBV-pos and 17 EBV-neg PTLD patients. Data are shown for (A) Naïve and memory subsets according to CD45RA and CCR7 expression, as well as (B) CD95⁺, (C)CD57⁺, (D) HLA-DR⁺ and (F) CD38⁺ surface markers within the CD3⁺CD8⁺ lymphocytes population. The density of (G) PD-1 and (H) TIM-3 expression on CD8⁺ T cell surface were measured as mean fluorescence intensity (MFI) by multiparametric flow cytometry in thawed PBMCs of 15 TC, 42 EBV-pos and 36 EBV-neg PTLD patients. Horizontal lines in dot-plots represent medians. Median values were compared between groups with a Kruskall Wallis test and Dunn's multiple comparison post-test. Individual measures are represented as blue squares (■) for TCs, green circles (●) for EBV-positive PTLDs and orange triangles (▲) for EBV-negative PTLDs.

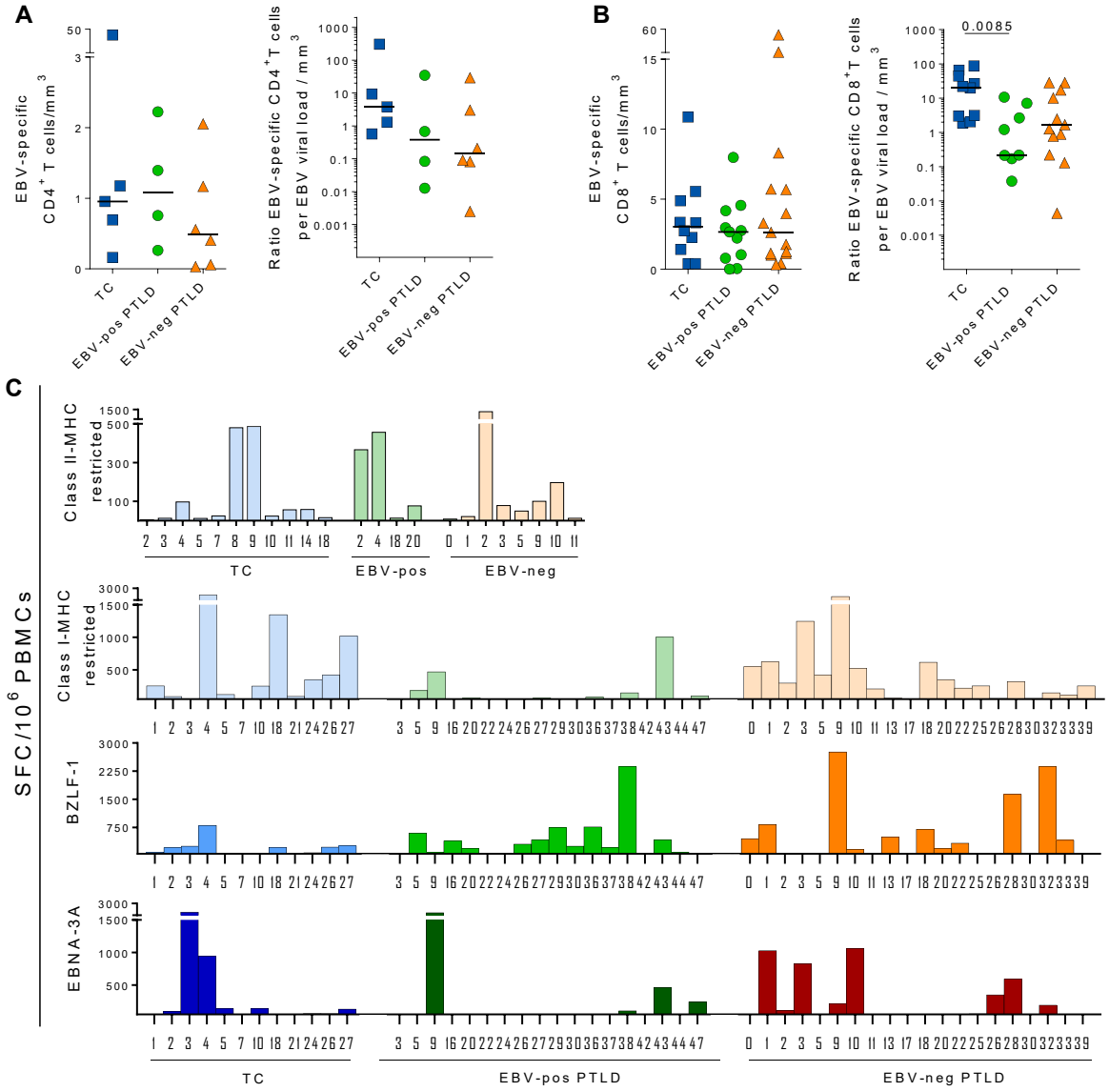

Supplemental Figure 8. Complementary data on EBV-specific T cell responses from EBV-positive and EBV-negative PTLD patients and transplant controls (TC). (A-B) EBV-specific T cells at inclusion were dectected by intracellular cytokine staining (IFNγ or IL-2 or TNFα) with flow cytometry after PBMC stimulation with EBV peptides: BZLF-1 and HLA-restricted. The number of EBV-specific (A) $CD4^+$ or (B) $CD8^+$T cells /mm^3 were determined from absolute $CD3^+CD4^+$ lymphocyte counts at inclusion, then a ratio between the number of EBV-specific T cells and the number of international units (IU) of EBV DNA /mm^3 was calculated. Data are shown for 10 transplant controls, 13 EBV-positive PTLD and 15 EBV-negative PTLD patients, although only a small amount of those patients could be tested for EBV-specific $CD4^+$ T cells. Horizontal lines in dot-plots represent medians. Median values were compared between groups

with a Kruskall Wallis test and Dunn's multiple comparison post-test. Individual measures are represented as blue squares (■) for TCs, green circles (●) for EBV-positive PTLDs and orange triangles (▲) for EBV-negative PTLDs. (C) Sum of EBV-specific T cell responses detected by Elispot IFNγ against each peptide pool are shown for each patient as Spot-forming cells (SFC)/10^6PBMCs. Numbers in the horizontal axis correspond to patients individual ID by group.

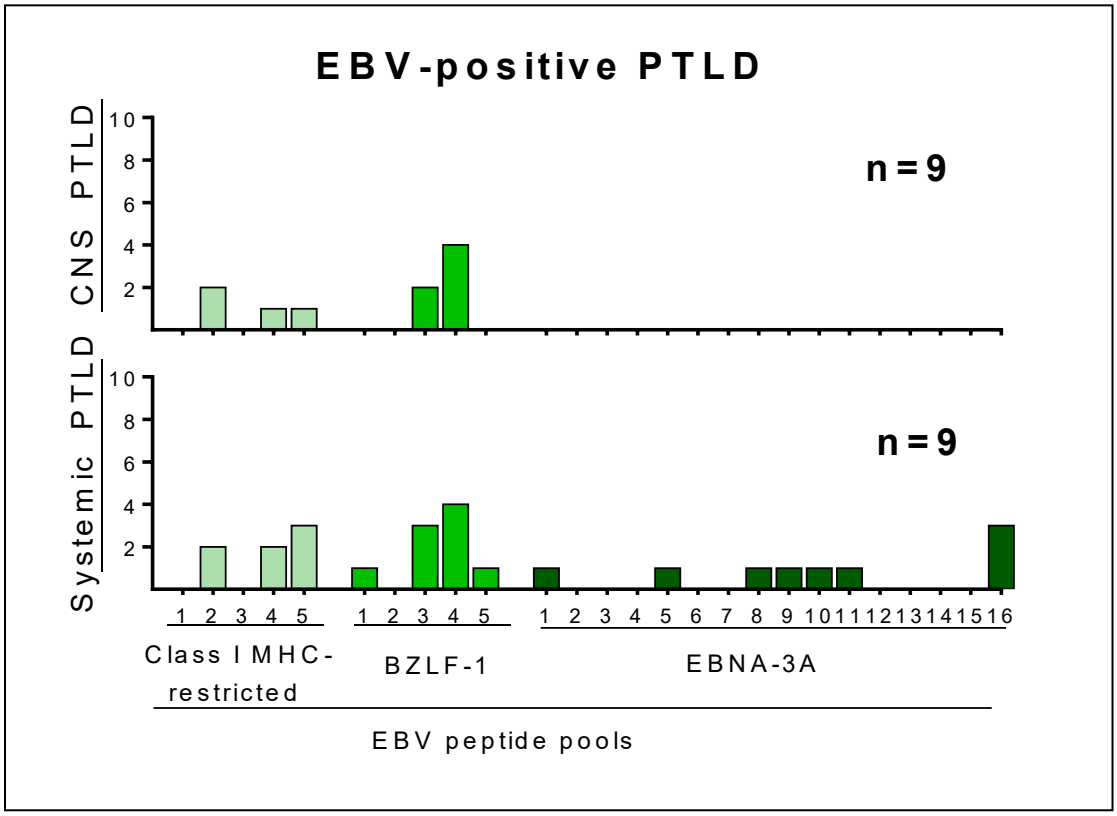

Supplemental Figure 9. Distribution of EBV-specific T cell responses in EBV-po PTLD patients according to disease localization. EBV-specific T-cell responses against different peptide pools of class-I MHC-restricted EBV-epitopes (n=5 pools), lytic BZLF-1 (n=5 pools) and latent EBNA-3A (n=16 pools) EBV proteins were measured in thawed PBMCs by ELISpot IFNγ assay. The number of patients with detectable responses (>50 spot forming cell units/10^6 PBMCs from triplicate tests after background subtraction) to each pool are shown for EBV-pos PTLDs with central nervous system (CNS) disease location (upper panel) or with systemic (nodal + extra-nodal) disease location (lower panel).